Heterochiral Recognition in Molecular and Macromolecular Pairs of Liquid Crystals Based on (R)- and (S)-2-Chloro-4-methylpentyl 4‘-[[8-(Vinyloxy)octyl)oxy]biphenyl-4-carboxylate] E...

ARTICLE *in* CHEMISTRY OF MATERIALS · JUNE 1999

Impact Factor: 8.35 · DOI: 10.1021/cm990083m

3 AUTHORS, INCLUDING:

Alexandru D Asandei
University of Connecticut
65 PUBLICATIONS **1,196** CITATIONS

Heterochiral Recognition in Molecular and Macromolecular Pairs of Liquid Crystals Based on (*R*)- and (*S*)-2-Chloro-4-methylpentyl 4′-[[8-(Vinyloxy)octyl)oxy]biphenyl-4-carboxylate] Enantiomers

V. Percec,* H. Oda, and A. D. Asandei

Roy & Diana Vagelos Laboratories, Department of Chemistry, University of Pennsylvania, Philadelphia, Pennsylvania 19104-6323

Received February 5, 1999. Revised Manuscript Received May 24, 1999

(*R*)-2-Chloro-4-methylpentyl 4′-[[11-(vinyloxy)undecanyl]oxy]biphenyl-4-carboxylate [(*R*)-**11**] (*R* > 95%) and (*S*)-2-chloro-4-methylpentyl 4′-[[11-(vinyloxy)undecanyl]oxy]biphenyl-4-carboxylate [(*S*)-**11**] (*S* > 95%) enantiomers and their corresponding homopolymers and copolymers with well-defined molecular weight and narrow molecular weight distribution were synthesized and characterized. The phase behavior of (*R*)-**11** and poly[(*R*)-**11**] are identical to those of (*S*)-**11** and poly[(*S*)-**11**]. Both monomers display a monotropic S_A phase and a crystalline phase, while the corresponding polymers display an enantiotropic S_A phase, monotropic S_C* (S_1) and S_2 (unidentified smectic) phases, and a crystalline phase. The two enantiomeric structural units derived from the two enantiomers are miscible in all mesophases except the S_1 phase of the polymer mixtures with DP > 10 where the S_1 phase is observed only in the high optical purity regions (mole fraction ≤ 0.2 and ≥ 0.8) and is replaced with another smectic (S_3) phase in the mol fraction range of 0.3−0.7. In the polymer mixtures with DP < 10 and in the copolymers, the S_1 phase showed a continuous dependence on the mixture compositions. The S_A−I transition and the K−S_A or K−I transition of the monomer mixtures are with 1.0 °C and 3.3−5.2 °C higher, respectively, in the 50/50 mixture than the theoretical value expected for an ideal solution, demonstrating the presence of chiral molecular recognition between the two enantiomers in both their S_A and crystalline phases. Positive deviations from the ideal values are also observed for the S_A−I (0.5 °C), S_2−S_3 (2.9−4.6 °C), and K−S_C* (4.7 °C) transition temperatures of the polymer mixtures. An optimum molecular weight that gives the largest chiral recognition effect is observed for each transition. The S_1−S_A or S_3−S_A transitions of the polymer mixtures and copolymers showed negative deviations from the ideal values (1.0−1.7 °C), indicating the nonideal solution behavior of the enantiomeric structural units in the S_1 and S_3 phases.

Introduction

The relationship between molecular structure and mechanism responsible for the manifestation of the chiral molecular recognition is very complex and, with the exception of the 2D case of Langmuir monolayers,[1] has not yet been quantitatively described in neither experiment or theory. Chiral molecular recognition[2] refers to the preferential selection by a chiral host of only one chiral guest from a mixture. The process is favored by steric or interactional complementarity, large contact areas, multiplicity of the interaction sites and strength of the interaction. In the case of enantiomers, chiral recognition is due to heterochiral complementary interactions and is observed in the phase diagrams of the binary mixtures of enantiomers as a positive deviation from the ideal solution behavior.

While there is a significant number of reports on the influence of chirality on the phase transitions of chiral low molar mass liquid crystals,[3−6] chiral molecular recognition was observed only in very few cases of layered phases of enantiomeric pairs of low molar mass liquid crystals[7−10] and very little understanding of the influence of structural parameters on its manifestation

* Corresponding author: telephone, 215-573-5527; fax, 215-573-7878; e-mail: percec@sas.upenn.edu.

(1) (a) Andelman, D.; de Gennes, P.-J. *C. R. Acad. Sci. Paris* **1988**, *307*, 233. (b) Andelman, D.; Orland, H. *J. Am. Chem. Soc.* **1993**, *115*, 12322.

(2) Lehn, J.-M. *Supramolecular Chemistry, Concepts and Perspectives*; VCH: Germany, 1995.

(3) (a) Jacques, J.; Collet, A.; Wilen, S. H. *Enantiomers, Racemates and Resolutions*; Krieger Publishing Co.: Malabar, 1991. (b) Leclercq, M.; Billard, J.; Jacques, J. *Mol. Cryst. Liq. Cryst.* **1969**, *8*, 367. (c) Bahr, C. H.; Heppke, G.; Sabaschus, B. *Ferroelectrics* **1988**, *84*, 103. (d) Bahr, C. H.; Heppke, G.; Sabaschus, B. *Liq. Cryst.* **1991**, *9*, 31.

(4) (a) Yamada, Y.; Mori, K.; Yamamoto, N.; Hayashi, H.; Nakamura, K.; Yamawaki, M.; Orihara, H.; Ishibashi, Y. *Jpn. J. Appl. Phys.* **1989**, *28*, L1606. (b) Takezoe, H.; Lee, J.; Chandani, A. D. L.; Gorecka, E.; Ouchi, Y.; Fukuda, A.; Terashima, K.; Furukawa, K. *Ferroelectrics* **1991**, *114*, 187. (c) Takezoe, H.; Fukuda, A.; Ikeda, A.; Takanishi, Y.; Umemoto, T.; Watanabe, J.; Iwane, H.; Hara, M.; Itoh, K. *Ferroelectrics* **1991**, *122*, 167. (d) Goodby, J. W.; Chin, E. *Liq. Cryst.* **1988**, *3*, 1245. (e) Goodby, J. W.; Patel, J. S.; Chin, E. *J. Mater. Chem.* **1992**, *2*, 197. (f) Heppke, G.; Lötzsch, D.; Demus, D.; Diele, S.; Jahn, K.; Zaschke, H. *Mol. Cryst. Liq. Cryst.* **1991**, *208*, 9.

10.1021/cm990083m CCC: $18.00
Published on Web 06/30/1999

Scheme 1. Synthesis of Monomers (*R*)-11 and (*S*)-11

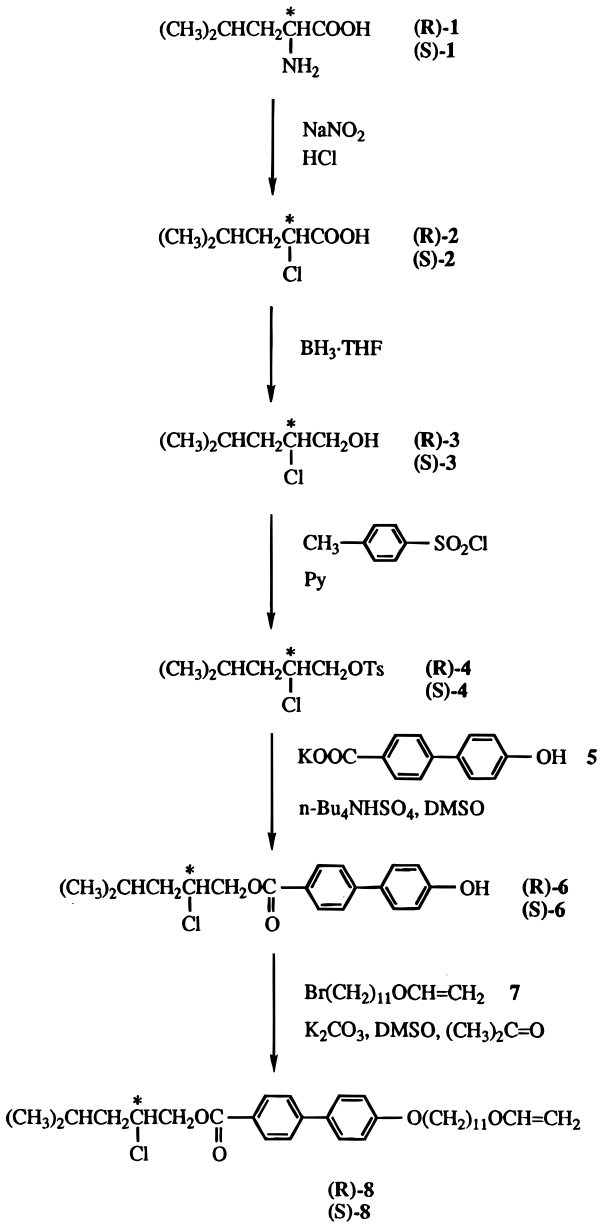

is available. With few exceptions[11] molecular recognition in enantiomeric and diastereomeric pairs of macromolecular liquid crystals has not been studied in great detail, mainly because of the lack of the techniques available to synthesize enantiomeric and diastereomeric pairs of liquid crystalline polymers with well-controlled molecular weight and narrow molecular weight distribution.

We are presently investigating[12] the effect of structural variables such as the nature (polarity and size) of the substituents at the chiral center and the molecular weight of the side chain liquid crystalline polymers derived from pairs of enantiomeric[12b,c,h] and diastereomeric[12a,d] monomers on the extent of chiral recognition in their binary mixtures. The assumption for this research is that the steric environment around the chiral center has a strong effect on the chiral molecular recognition and is inspired by theoretical predictions made for the case of Langmuir monolayers.[1] In this context, we have systematically investigated a series of

Scheme 2. Cationic Polymerization of (*R*)-11 and (*S*)-11

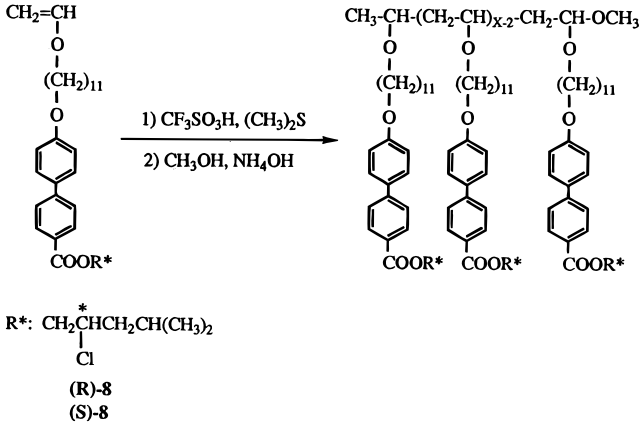

enantiomeric vinyl ether monomers containing a biphenyloxy carboxylate mesogenic unit linked to the vinyl ether via an octyl or undecanyl aliphatic chain. The chiral ester unit is derived from (*R*)- or (*S*)-leucine where the $-NH_2$ group was converted to either a $-F$,[12c] $-Cl$,[12b] or $-CN$[12h] group. The living cationic polymerization of the monomers provides access to polymers with well-defined molecular weight and narrow molecular weight distribution while tolerating the presence of various functional groups on the monomer.[13]

(5) (a) Goodby, J. W.; Waugh, M. A.; Stein, S. M.; Chin, E.; Pindak, R.; Patel, J. S. *J. Am. Chem. Soc.* **1989**, *111*, 8119. (b) Slaney, A. J.; Goodby, J. W. *Liq. Cryst.* **1991**, *9*, 849. (c) Goodby, J. W.; Nishiyama, I.; Slaney, A. J.; Booth, C. J.; Toyne, K. J. *Liq. Cryst.* **1993**, *14*, 37. (d) Nguyen, H. T.; Twieg, R. J.; Nabor, M. F.; Isaert, N.; Destrade, C. *Ferroelectrics* **1991**, *121*, 187. (e) Navailles, L.; Nguyen, H. T.; Barois, P.; Destrade, C.; Isaert, N. *Liq. Cryst.* **1993**, *15*, 479.

(6) (a) Levelut, A. M.; Germain, C.; Keller, P.; Liebert, L.; Billard, J. *J. Phys., Paris* **1983**, *44*, 623. (b) Keller, P. *Mol. Cryst. Liq. Cryst. Lett.* **1984**, *102*, 295. (c) Billard, J.; Dahlgren, A.; Flatischler, K.; Lagerwall, S. T.; Otterholm, B. J. *Phys., Paris* **1985**, *46*, 1241. (d) Heppke, G.; Kleineberg, P.; Lötzsch, D. *Liq. Cryst.* **1993**, *14*, 67.

(7) (a) Goodby, J. W.; Waugh, M. A.; Stein, S. M.; Chin, E.; Pindak, R.; Patel, J. S. *J. Am. Chem. Soc.* **1989**, *111*, 8119. (b) Slaney, A. J.; Goodby, J. W. *Liq. Cryst.* **1991**, *9*, 849. (c) Goodby, J. W.; Nishiyama, I.; Slaney, A. J.; Booth, C. J.; Toyne, K. J. *Liq. Cryst.* **1993**, *14*, 37. (d) Goodby, J. W.; Chin, E. *Liq. Cryst.* **1988**, *3*, 1245. (e) Goodby, J. W.; Patel, J. S.; Chin, E. *J. Mater. Chem.* **1992**, *2*, 197.

(8) (a) Levelut, A. M.; Germain, C.; Keller, P.; Liebert, L.; Billard, J. *J. Phys., Paris* **1983**, *44*, 623. (b) Keller, P. *Mol. Cryst. Liq. Cryst. Lett.* **1984**, *102*, 295. (c) Billard, J.; Dahlgren, A.; Flatischler, K.; Lagerwall, S. T.; Otterholm, B. J. *Phys., Paris* **1985**, *46*, 1241. (d) Heppke, G.; Kleineberg, P.; Lötzsch, D. *Liq. Cryst.* **1993**, *14*, 67. (e) Nguyen, H. T.; Twieg, R. J.; Nabor, M. F.; Isaert, N.; Destrade, C. *Ferroelectrics* **1991**, *121*, 187. (f) Heppke, G.; Lötzsch, D.; Demus, D.; Diele, S.; Jahn, K.; Zaschke, H. *Mol. Cryst. Liq. Cryst.* **1991**, *208*, 9.

(9) (a) Leclercq, M.; Billard, J.; Jacques, J. *Mol. Cryst. Liq. Cryst.* **1969**, *8*, 367. (b) Bahr, CH.; Heppke, G.; Sabaschus, B. *Ferroelectrics* **1988**, *84*, 103. (c) Bahr, CH.; Heppke, G.; Sabaschus, B. *Liq. Cryst.* **1991**, *9*, 31.

(10) (a) Yamada, Y.; Mori, K.; Yamamoto, N.; Hayashi, H.; Nakamura, K.; (b) Yamawaki, M.; Orihara, H.; Ishibashi, Y. *Jpn. J. Appl. Phys.* **1989**, *28*, L1606. (c) Takezoe, H.; Lee, J.; Chandani, A. D. L.; Gorecka, E.; Ouchi, Y.; Fukuda, A.; Terashima, K.; Furukawa, K. *Ferroelectrics* **1991**, *114*, 187. (d) Takezoe, H.; Fukuda, A.; Ikeda, A.; Takanishi, Y.; Umemoto, T.; Watanabe, J.; Iwane, H.; Hara, M.; Itoh, K. *Ferroelectrics* **1991**, *122*, 167.

(11) (a) Li, L.-S.; Stupp, S. I. *Macromolecules* **1995**, *28*, 2618. (b) Stupp, S. I.; Son, S.; Lin, H. C.; Li, L. S. *Science* **1993**, *259*, 59. (c) Stupp, S. I.; Son, S.; Lin, H. C.; Li, L. S.; Keser, M. *J. Am. Chem. Soc.* **1995**, *117*, 5212.

(12) (a) Percec, V.; Oda, H.; Rinaldi, P. L.; Hensley, D. R. *Macromolecules* **1994**, *27*, 12. (b) Percec, V.; Oda, H. *Macromolecules* **1994**, *27*, 4454. (c) Percec, V.; Oda, H. *Macromolecules* **1994**, *27*, 5821. (d) Percec, V.; Oda, H. *J. Macromol. Sci., Chem.* **1995**, *A32*, 1531. (e) Percec, V.; Oda, H. *J. Mater. Chem.* **1995**, *5*, 1125. (f) Percec, V.; Oda, H. *J. Polym. Sci.: Part A: Polym. Chem.* **1995**, *33*, 2359. (g) Percec, V.; Oda, H. *J. Mater. Chem.* **1995**, *5*, 1115. (h) Percec, V.; Zheng, Q.; Asandei, A. D. Submitted to publication.

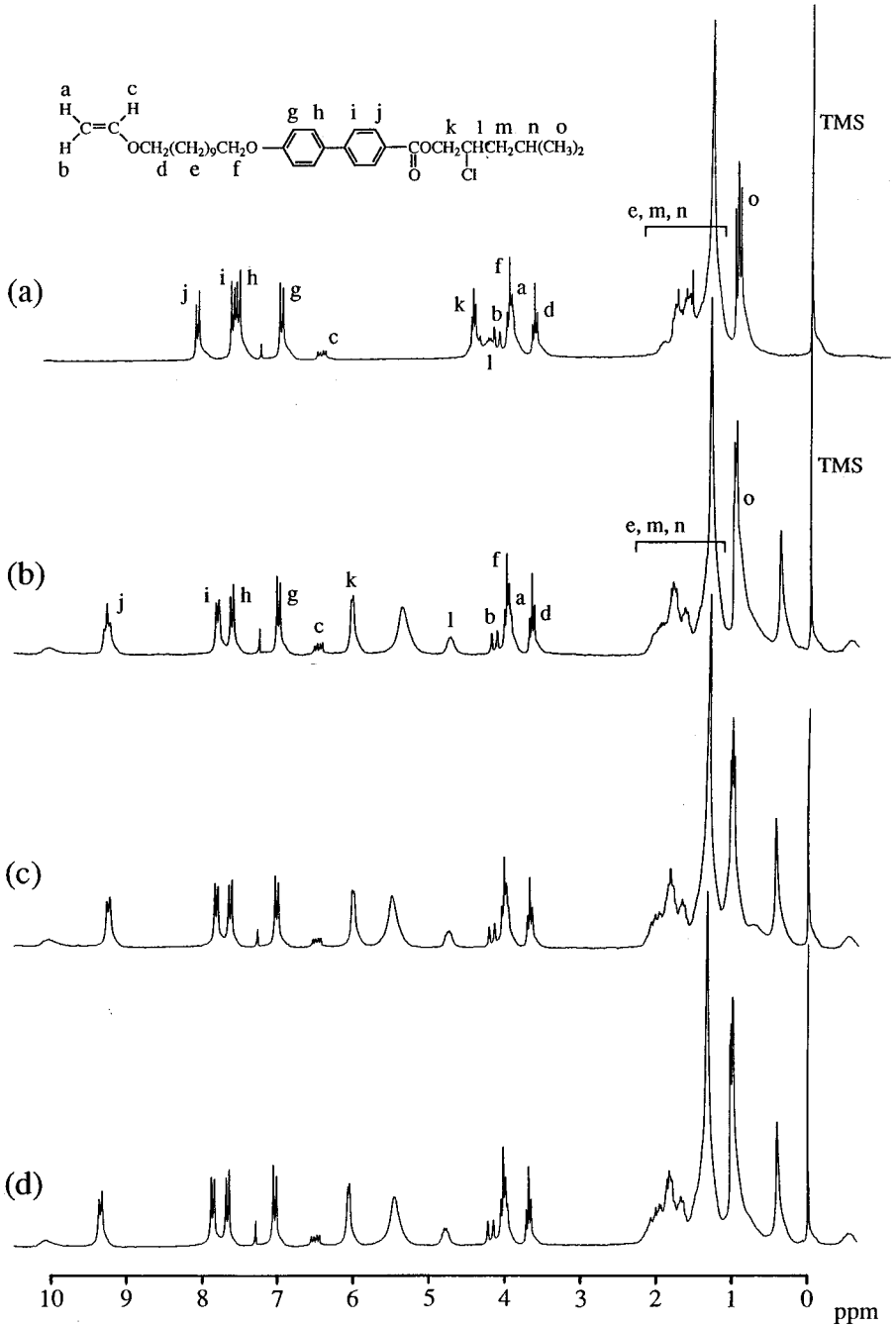

Figure 1. ^{1}H NMR spectra of monomers: (a) (*R*)-**11**; (b) (*R*)-**11**/(*S*)-**11** (50/50 mixture) with Eu(hfc)$_3$; (c) (*R*)-**11** with Eu(hfc)$_3$; and (d) (*S*)-**11** with Eu(hfc)$_3$.

The chiral molecular recognition effect is detected by comparing the experimental dependence of the transition temperatures of mixtures with different compositions with the theoretical values predicted by the Schröder−van Laar equation for ideal behavior.[14] Formation of a nonideal solution with a positive deviation (upward curvature) of the dependence of the transition temperatures on composition is indicative of a heterochiral recognition effect. We have observed chiral molecular recognition in the $S_A^{12a-c,h}$ or $S_C^{*12c,h}$ phases of the mixtures of monomers and of polymers and found that the extent of chiral molecular recognition is dependent on the molecular weight in the case of liquid crystalline polymer pairs.[12b,c] However, each individual system provides different and unique mesophase behavior and, consequently, a comprehensive comparison and isolation of individual contributions to the chiral recognition effect is difficult to make in a quantitative manner.

The first goal of this paper is to describe the synthesis and the living cationic polymerization of (*R*)-2-chloro-4-methylpentyl 4′-[[11-(vinyloxy)undecanyl]oxy]biphenyl-4-carboxylate [(*R*)-**11**] and (*S*)-2-chloro-4-methyl-

(13) (a) Percec, V.; Tomazos, D. *Adv. Mater.* **1992**, *4*, 548. (b) Percec, V.; Zheng, Q.; Lee, M. *J. Mater. Chem.* **1991**, *1*, 611. (c) Percec, V.; Zheng, Q.; Lee, M. *J. Mater. Chem.* **1991**, *1*, 1015. (d) Percec, V.; Zheng, Q. *J. Mater. Chem.* **1992**, *2*, 475. (e) Percec, V.; Zheng, Q. *J. Mater. Chem.* **1992**, *2*, 1041.

(14) (a) Van Hecke, G. R. *J. Phys. Chem.* **1979**, *83*, 2344. (b) Achard, M. F.; Mauzac, M.; Richard, H.; Sigaud, G.; Hardouin, F. *Eur. Polym. J.* **1989**, *25*, 593.

Table 1. Characterization of the Binary Mixtures of Monomers (*R*)-11 with (*S*)-11

	phase transitions (°C) and corresponding enthalpy changes (kcal/mol)[a]	
(*R*)-**11**/(*S*)-**11** (mol)/(mol)	heating	cooling
0/100	K 47.0 (12.78) I K 38.6 (0.22) K 46.9 (12.67) I	I 20.5 (−1.06) S_A 8.8 (−6.96) K
11.7/88.3	K 48.6 (13.03) I K 48.1 (12.36) I	I 21.2 (−1.08) S_A 12.6 (−8.50) K
20.2/79.8	K 48.9 (13.22) I K 48.3 (12.65) I	I 21.6 (−1.09) S_A 14.0 (−8.73) K
39.9/60.1	K 49.7 (13.30) I K 49.6 (13.05) I	I 22.0 (−1.10) S_A 13.4 (−8.65) K
44.0/56.0	K 50.3 (13.53) I K 50.0 (13.26) I	I 22.0 (−1.12) S_A 13.0 (−8.61) K
50.3/49.7	K 50.1 (13.59) I K 50.0 (13.29) I	I 22.0 (−1.11) S_A 12.5 (−8.44) K
55.0/45.0	K 50.3 (13.41) I K 49.9 (13.08) I	I 22.0 (−1.11) S_A 12.9 (−8.50) K
60.4/39.3	K 50.2 (13.46) I K 49.9 (13.17) I	I 22.0 (−1.11) S_A 13.0 (−8.54) K
80.1/19.9	K 48.3 (13.33) I K 47.8 (12.72) I	I 22.1 (−1.13) S_A 11.3 (−8.37) K
89.8/10.2	K 47.5 (13.06) I K 47.1 (12.60) I	I 21.8 (−1.12) S_A 9.6 (−7.66) K
100/0	K 46.6 (12.99) I K 38.8 (3.91) K 40.0 (−1.17) K 46.2 (8.28) I	I 21.5 (−1.09) S_A 5.6 (−6.58) K

[a] Data on the first line are from first heating and cooling scans. Data on the second line are from second heating scan. Heating and cooling rates are 10 °C/min.

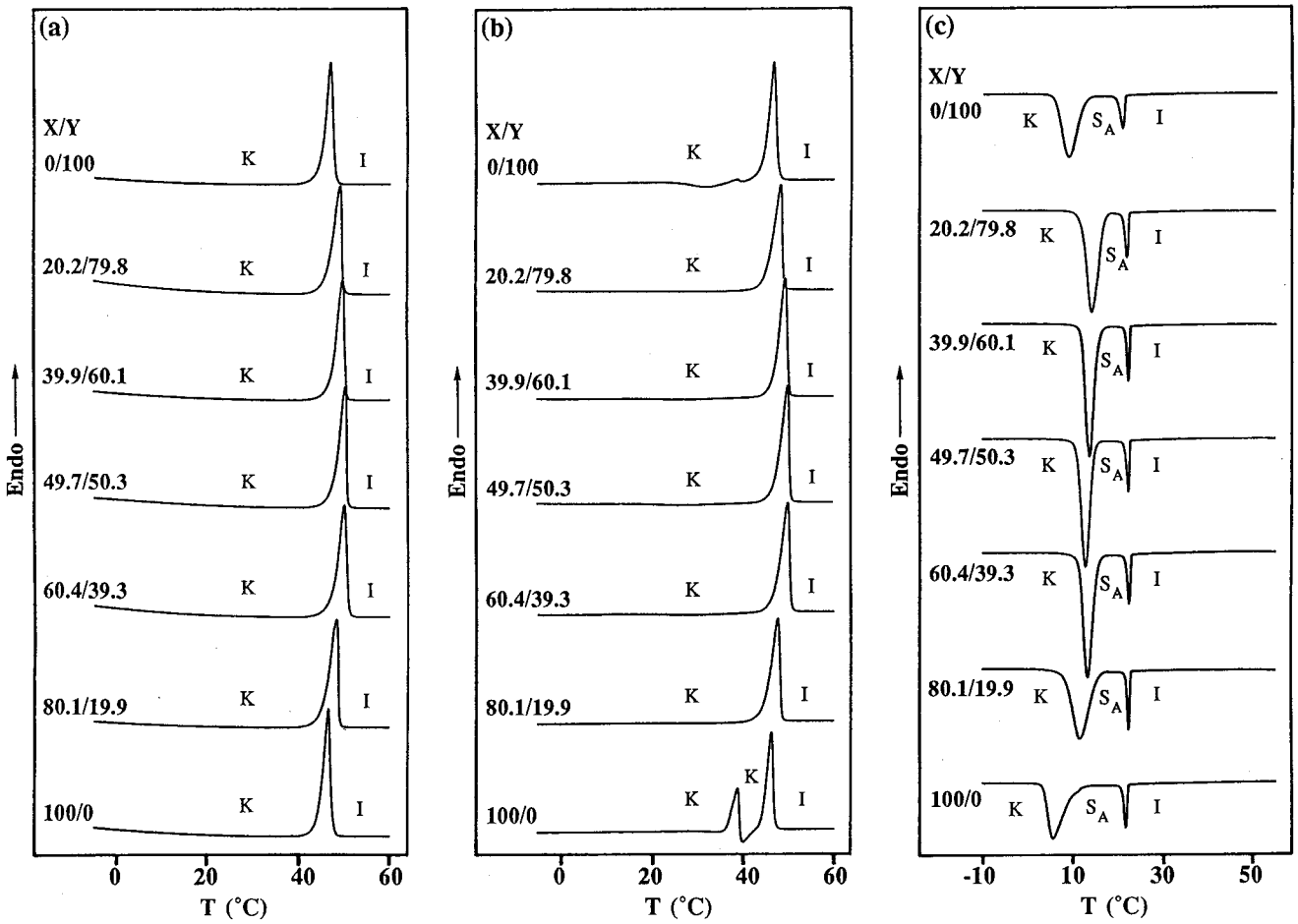

Figure 2. DSC thermograms (10 °C/min) of the binary mixtures of monomer (*R*)-**11** (X) with monomer (*S*)-**11** (Y): (a) first heating scans; (b) second heating scans; and (c) first cooling scans.

pentyl 4′-[[11-(vinyloxy)undecanyl]oxy]biphenyl-4-carboxylate [(*S*)-**11**] enantiomers. The second goal is to investigate the phase behavior and chiral molecular recognition effects in binary mixtures of monomers and polymers, and in copolymers and to compare them with similar systems based on (*R*)- and (*S*)-2-chloro-4-methylpentyl 4′-[[8-(vinyloxy)octyl]oxy]biphenyl-4-carboxylate enantiomers.[12b]

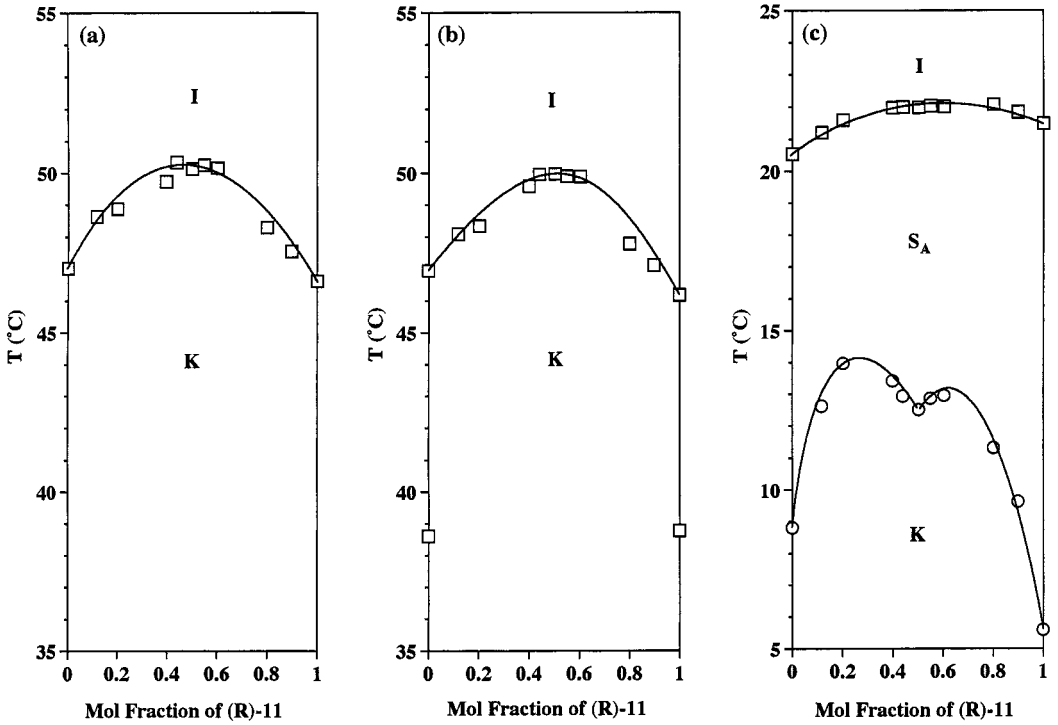

Figure 3. Dependence of phase transition temperatures on the composition of the binary mixtures of (*R*)-**11** with (*S*)-**11**: (a) data from the first heating scans; (b) data from the second heating scans; and (c) data from the first cooling scans.

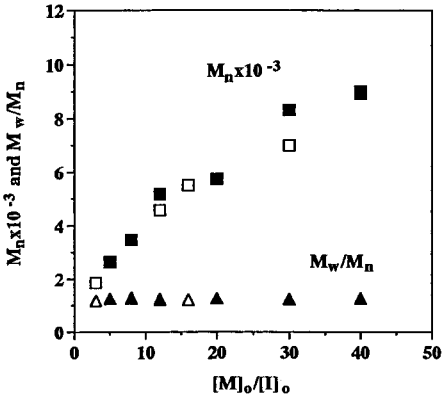

Figure 4. Dependence of the number-average molecular weight (M_n) and polydispersity (M_w/M_n) of poly[(*R*)-**11**] (open symbols) and poly[(*S*)-**11**] (closed symbols) determined by GPC on the $[M]_o/[I]_o$ ratio.

Results and Discussion

Synthesis of Monomers and Polymers and Determination of Their Optical Purities. We have previously reported[12b] the synthesis and living cationic polymerization of (*R*)- and (*S*)-2-chloro-4-methylpentyl 4′-[[8-(vinyloxy)octyl]oxy]biphenyl-4-carboxylate. Monomers (*R*)- and (*S*)-**11** were synthesized by the same method except that an undecanyl alkyl group was used as spacer instead of an octyl alkyl group. The reaction pathway is outlined in Scheme 1.

The homopolymerizations of (*R*)-**11** and (*S*)-**11** are presented in Scheme 2. All polymerizations were carried out at 0 °C in CH_2Cl_2 by a living cationic polymerization technique using $CF_3SO_3H/(CH_3)_2S$ as an initiation system. Previous work in our[15] and other[16] laboratories has shown that the CF_3SO_3H initiated polymerization of vinyl ethers in the presence of a Lewis base such as $(CH_3)_2S$ affords well-defined polymers with controlled molecular weights and narrow polydispersities. The polymerization mechanism is discussed in detail in previous publications.[13,15,17]

The optical purities of monomers (*R*)- and (*S*)-**11**, and of the corresponding polymers poly[(*R*)-**11**] and poly[(*S*)-**11**] were determined as previously described.[12] Figure 1a presents the ^{1}H NMR spectrum of monomer (*R*)-**11**. Figure 1b presents the ^{1}H NMR spectrum of the 50/50 mixture between (*R*)- and (*S*)-**11** with a chiral shift reagent tris[3-(heptafluoropropylhydroxymethylene)−(+)-camphorato]europium(III) derivative [Eu(hfc)$_3$]. Parts c and d of Figure 1 present the ^{1}H NMR spectra of pure (*R*)- and (*S*)-**11** with Eu(hfc)$_3$, respectively. These results are similar to those previously reported[12] and the estimated optical purities for (*R*)- and (*S*)-**11** are higher than 95%. The optical purity of homopolymers could not be directly determined because the polymers showed broadened signals even in the absence of the shift reagent. However, our previous experiments have demonstrated that the chiral center of the monomer is insensitive to the cationic polymerization conditions and subsequently, the original optical purity of the monomer remains unchanged during the polymerization process.[12]

Phase Behavior of Mixtures of Monomers, Mixtures of Polymers and of the Copolymers. *Monomer Mixtures.* The (*R*)-**11** and (*S*)-**11** enantiomeric monomers were mixed in various compositions and the phase behavior of their mixtures was investigated by DSC. Mixtures were prepared by dissolving the two monomers

(15) (a) Percec, V.; Lee, M.; Jonsson, H. *J. Polym. Sci: Part A: Polym. Chem.* **1991**, *29*, 327. (b) Percec, V.; Lee, M. *Macromolecules* **1991**, *24*, 1017. (c) Percec, V.; Lee, M.; Rinaldi, P.; Litman, V. E. *J. Polym. Sci: Part A: Polym. Chem.* **1992**, *30*, 1213.

(16) (a) Cho, C. G.; Feit, B. A.; Webster, O. W. *Macromolecules* **1990**, *23*, 1918. (b) Cho, C. G.; Feit, B. A.; Webster, O. W. *Macromolecules* **1992**, *25*, 2081. (c) Lin, C. H.; Matyjaszewski, K. *Polym. Prepr., Am. Chem. Soc. Div. Polym. Chem.* **1990**, *31*, 599.

(17) Percec, V.; Zheng, Q. *J. Mater. Chem.* **1992**, *2*, 1041.

Table 2. Cationic Polymerization of (*R*)-2-Chloro-4-methylpentyl 4′-[[11-(Vinyloxy)undecanyl]oxy]biphenyl-4-carboxylate ((*R*)-11) and Characterization of the Resulting Polymers[a]

sample no.	$[M]_o/[I]_o$	polymer yield (%)	$M_n \times 10^{-3}$	M_w/M_n	DP	phase transitions (°C) and corresponding enthalpy changes (kcal/mru)[b] heating	cooling
1	3	42.2	1.86	1.18	4	K 33.7 (3.18) S_A 62.4 (1.21) I K 24.9 (2.58) S_1 39.3 (†[c]) S_A 64.0 (1.20) I	I 58.6 (−1.29) S_A 35.6 (−0.06) S1 2.3 (−2.23) K
2	8	61.3	3.47	1.26	7	K 39.4 (3.08) S_A 74.8 (1.08) I K 29.3 (1.99) S_1 42.4 (†[c]) S_A 75.1 (1.10) I	I 70.3 (−1.10) S_A 38.9 (−0.08) S_1 4.5 (−1.17) K
3	12	67.5	4.57	1.24	9	K 42.3 (3.45) K 54.9 (†[c]) S_A 82.6 (1.03) I K 33.7 (0.59) K 46.5 (1.36) S_A 82.9 (1.02) I	I 77.4 (−1.02) S_A 42.5 (−0.09) S_1 15.0 (−1.36) K
4	16	68.6	5.51	1.21	10	K 42.6 (3.40) K 61.1 (†[c]) S_A 87.4 (0.97) I K 57.0 (1.88) S_A 87.7 (0.98) I	I 81.9 (−0.98) S_A 44.1 (−0.08) S_1 21.2 (−1.46) K
5	30	78.1	7.01	1.24	13	K 42.8 (†[c]) K 65.2 (3.52) S_A 91.7 (0.93) I K 62.7 (2.24) S_A 92.0 (0.91) I	I 86.3 (−0.92) S_A 46.0 (−0.08) S_1 31.0 (−0.34) S_2 27.1 (−1.28) K
6	40	82.3	9.01	1.27	17	K 43.2 (†[c]) K 66.2 (3.41) S_A 94.9 (0.89) I K 61.9 (2.04) S_A 95.1 (0.89) I	I 89.1 (−0.89) S_A 46.8 (−0.07) S_1 33.8 (−0.35) S2 28.5 (−1.18) K

[a] Polymerization temperature: 0 °C; polymerization solvent, methylene chloride; $[M]_o = 0.224$; $[Me_2S]_o/[I]_o = 10$; polymerization time, 1 h. [b] Data on the first line are from first heating and cooling scans. Data on the second line are from second heating scan. Heating and cooling rates are 10 °C/min. [c] Overlapped peak.

Table 3. Cationic Polymerization of (S)-2-Chloro-4-methylpentyl-4′-(11-vinyloxyundecanyloxy)Biphenyl-4-carboxylate ((S)-11) and Characterization of the Resulting Polymers[a]

sample no.	$[M]_o/[I]_o$	polymer yield (%)	$M_n \times 10^{-3}$	M_w/M_n	DP	phase transitions (°C) and corresponding enthalpy changes (kcal/mru)[b] heating	cooling
1	5	23.7	2.64	1.25	5	K 36.6 (3.20) S_A 70.7 (1.20) I K 26.3 (2.07) S_1 39.8 (†[c]) S_A 71.4 (1.23) I	I 66.1 (−1.23) S_A 36.0 (−0.07) S_1 3.0 (−1.46) K
2	8	68.2	3.47	1.28	7	K 39.0 (3.06) S_A 72.5 (1.06) I K 28.8 (1.68) S_1 40.2 (†[c]) S_A 72.6 (1.07) I	I 67.6 (−1.08) S_A 36.8 (−0.08) S_1 2.5 (−1.00) K
3	12	60.0	5.17	1.20	10	K 42.7 (3.39) K 58.1 (†[c]) S_A 84.0 (0.99) I K 31.7 (0.12) K 47.5 (1.54) S_A 84.4 (0.98) I	I 78.7 (−0.99) S_A 42.2 (−0.08) S_1 15.8 (−1.22) K
4	20	68.6	5.75	1.26	11	K 43.6 (3.53) K 60.7 (†[c]) S_A 86.8 (0.96) I K 59.2 (2.40) S_A 87.3 (0.95) I	I 81.7 (−0.97) S_A 43.8 (−0.07) S_1 23.2 (†[c]) S_2 21.3 (−1.42) K
5	30	81.8	8.33	1.23	16	K 45.2 (1.07) K 67.0 (2.42) S_A 93.8 (0.89) I K 59.6 (2.38) S_A 93.7 (0.88) I	I 88.0 (−0.88) S_A 46.5 (−0.07) S_1 32.9 (−0.34) S_2 27.9 (−1.16) K
6	40	79.6	8.94	1.25	17	K 44.3 (†[c]) K 65.6 (3.30) S_A 93.7 (0.87) I K 59.5 (1.94) S_A 94.0 (0.87) I	I 88.1 (−0.88) S_A 46.3 (−0.07) S_1 32.7 (−0.34) S_2 27.7 (−1.10) K

[a] Polymerization temperature: 0 °C; polymerization solvent, methylene chloride; $[M]_o = 0.224$; $[Me_2S]_o/[I]_o = 10$; polymerization time, 1 h. [b] Data on the first line are from first heating and cooling scans. Data on the second line are from second heating scan. Heating and cooling rates are 10 °C/min. [c] Overlapped peak.

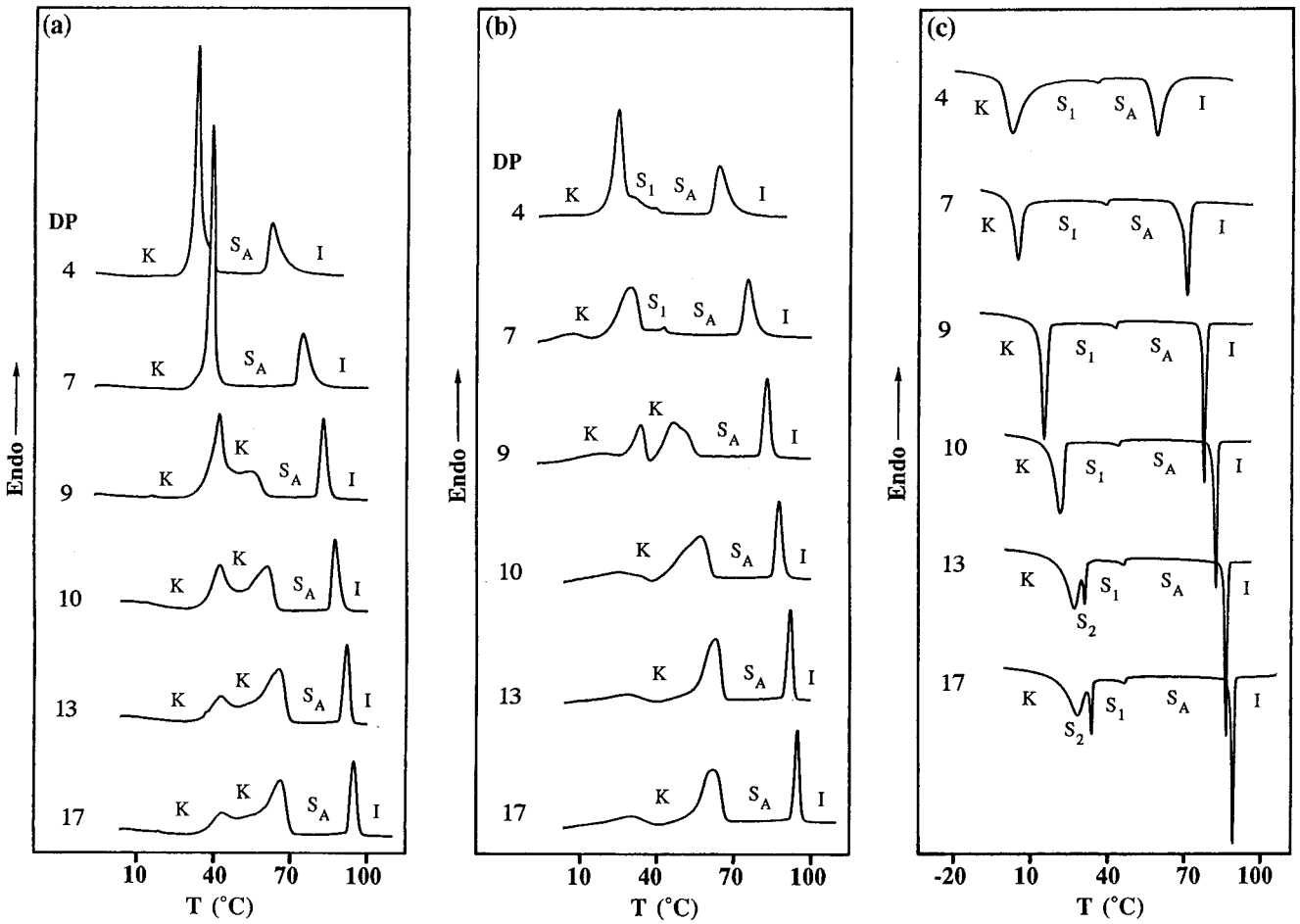

Figure 5. DSC thermograms (10 °C/min) of poly[(*R*)-**11**] with different DP: (a) first heating scans; (b) second heating scans; and (c) first cooling scans.

in CH_2Cl_2 followed by evaporation of the solvent under vacuum. The thermal transition temperatures and the corresponding enthalpy changes are summarized in Table 1. DSC thermograms of the monomer mixtures are presented in Figure 2 and the corresponding phase diagrams are shown in Figure 3.

The small difference between the transition temperatures of the enantiomers are due to the slight differences in their enantiomeric excesses (ee). However, both are > 95% ee. For all compositions a crystalline phase is observed on the first and subsequent heating DSC scans while a monotropic S_A phase and a crystalline phase is observed on the cooling DSC scan. The dependence of the crystalline to isotropic (K−I) transition temperature on composition shows a nonideal solution behavior induced by heterochiral interactions with an upward curvature and a positive deviation of up to 3.3 °C from the theoretical ideal value calculated calculated using the Schröder−van Laar equation.[14] The same effect is observed on the second heating scan. On the cooling scan, the I−S_A transition also displays the positive curvature but with a smaller deviation of 1 °C from the calculated value. The dependence of the S_A−K transition temperature on composition is more complex showing that chiral recognition (positive deviation from the ideal behavior) occurs not only between the two enantiomers but between the racemate and each enantiomer as well. A positive deviation of up to 5.6 °C is observed for the 1:1 mixture of enantiomers whereas positive deviations of up to 2.8 °C and, respectively, 3.8 °C are observed for the 1:1 mixture of the racemic with the *S* and respectively *R* enantiomer. These results demonstrate that chiral molecular recognition is present between the two enantiomeric structural units of the monomers both in their crystalline and S_A phases.

Polymer−Polymer Mixtures. The characterization of poly[(*R*)-**11**] and poly[(*S*)-**11**] by gel permeation chromatography (GPC) and differential scanning calorimetry (DSC) is summarized in Tables 2 and 3, respectively. The low polymer yields are the result of the loss of polymer during purification. Relative number-average molecular weights of polymers determined by GPC exhibit a linear dependence on the initial molar ratio of monomer to initiator ($[M]_o/[I]_o$) as shown in Figure 4 and demonstrate that the $[M]_o/[I]_o$ ratio provides a good control of the polymer molecular weight. All polydispersities are less than 1.28. These features demonstrate the typical characteristics of the living polymerization mechanism. The absolute number-average molecular weights were difficult to determine by ^{1}H NMR spectroscopy from the chain ends of the polymer, owing to signal overlap.

The mesomorphic behavior of poly[(*R*)-**11**] and poly[(*S*)-**11**] was investigated by DSC and thermal optical polarized microscopy. Figures 5 and 6 present the DSC thermograms of poly[(*R*)-**11**] and poly[(*S*)-**11**] with various degrees of polymerization (DP). The phase behavior of the homopolymers was compared by superimposing

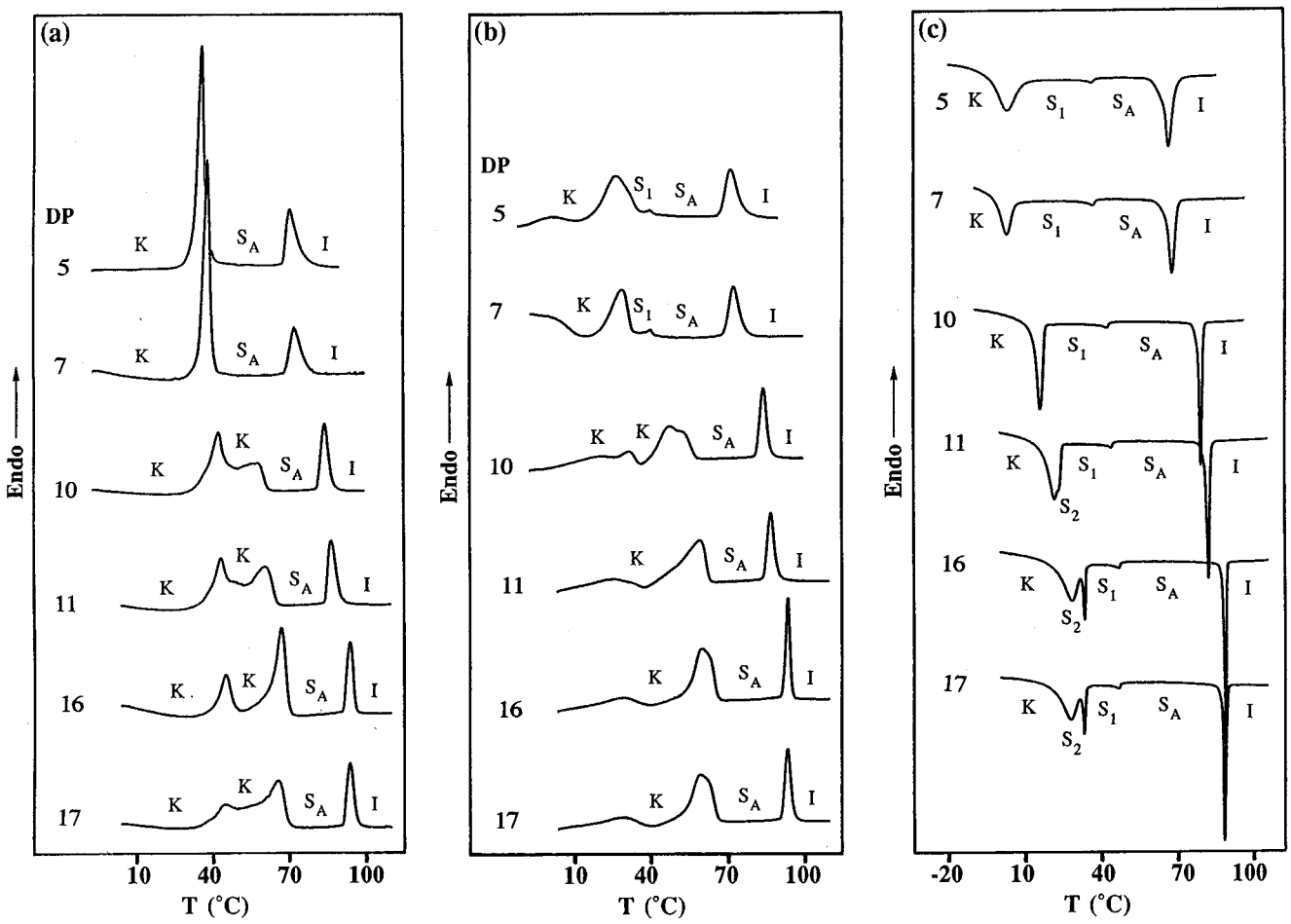

Figure 6. DSC thermograms (10 °C/min) of poly[(*S*)-**11**] with various DPs: (a) first heating scans; (b) second heating scans; and (c) first cooling scans.

the plots of the dependencies of their thermal transition temperatures as a function of DP in Figure 7. The phase behavior of poly[(*R*)-**11**] is identical to that of poly[(*S*)-**11**]. On the first heating scan, all polymers exhibit a crystalline phase which melts into a S_A phase. Polymers with DP ≤ 7 show one sharp crystalline melting peak, while polymers with DP > 7 show two broad crystalline melting peaks. In the polarized optical microscope analysis, the S_A phase of all polymers displays a clear focal conic texture. On the first cooling scan, a S_A and then a S_C*[12] (S_1) phase are observed. For DP ≥ 13, the S_C* is followed by an unidentified higher order monotropic smectic phase (S_2) and a crystalline phase. For DP < 13, the S_2 phase is not observed. On the second heating scan, all polymers display crystalline meltings and the S_A phase. For DP ≤ 7, the crystalline phase melts into the S_C* phase which is therefore enantiotropic up to DP ≤ 7 and monotropic for DP > 7. The S_A phase is enantiotropic for all DPs. As observed from Figure 7, all transition temperatures increase with DP (polymer effect).[12b] The I−S_A transition from the cooling scan is more sensitive to the effect of DP than the S_A−S_C* transition. As a consequence, the temperature range of the S_A phase increases with DP.

To obtain further information on the nature of the smectic phases displayed by these polymers, X-ray diffraction experiments were performed. The diffraction patterns of poly[(*R*)-**11**] (DP = 17.0) are presented in Figure 8. On the heating scan, below 70 °C, two well-resolved peaks are observed at $2\theta = 3.020°$ and 4.860°. The layer spacing calculated from the former peak is 29.3 Å and this value is smaller than the calculated side chain length of the polymer (31.6 Å). Above 70 °C, a strong diffraction signal is observed at $2\theta = 2.820°$, which corresponds to 31.3 Å of the layer spacing. This value is in good agreement with the calculated side chain length of the polymer. These results support the existence of the S_A phase and the tilted layered structure of the S_C* phase. In the DSC measurements, this polymer melted into an isotropic liquid at 95 °C (10 °C/min), whereas in the X-ray analysis (2.5 °C), the S_A layered structure was retained up to 100 °C and disappeared at 110 °C. As shown in Figure 8b, the small diffraction peak observed at $2\theta = 1.8°$ remains throughout the cooling scans. No other distinctive peaks are observed. This result may to suggest the formation of bi- or multilayer smectic structure.[18,19] A complementary X-ray analysis, including a small-angle scattering experiment, would be required to support this speculation.

(18) (a) Imrie, C. T.; Schleeh, T.; Karasz, F. E.; Attard, G. S. *Macromolecules* **1993**, *26*, 539. (b) Chiellini, E.; Galli, G.; Cioni, F.; Dossi, E.; Gallot, B. *J. Mater. Chem.* **1993**, *3*, 1065.

(19) (a) Kühnpast, K.; Springer, J.; Davidson, P.; Scherowsky, G. *Makromol. Chem.* **1992**, *193*, 3097. (b) Kühnpast, K.; Springer, J.; Scherowsky, G.; Giesselmann, F.; Zugenmaier, P. *Liq. Cryst.* **1993**, *14*, 861. (c) Davidson, P.; Kühnpast, K.; Springer, J.; Scherowsky, G. *Liq. Cryst.* **1993**, *14*, 901.

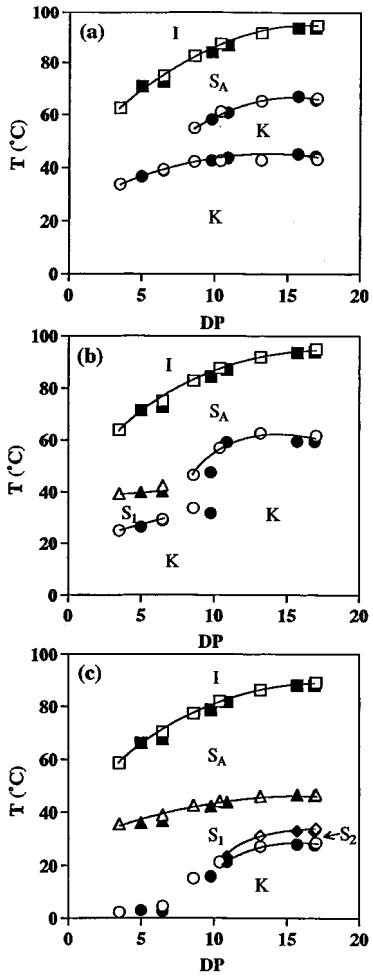

Figure 7. Dependence of phase transition temperatures on the degree of polymerization of poly[(*R*)-**11**] (open symbols) and poly[(*S*)-**11**] (closed symbols): (a) data from the first heating scans; (b) data from the second heating scans; and (c) data from the first cooling scans.

Three sets of binary mixtures between poly[(*R*)-**11**] and poly[(*S*)-**11**] with different molecular weights were prepared and their phase behavior was investigated. The molecular weights and polydispersities of the polymers employed in this miscibility study were as follows: polymer mixture I, poly[(*R*)-**11**] with DP = 7, M_w/M_n = 1.26 and poly[(*S*)-**11**] with DP = 7, M_w/M_n = 1.28; polymer mixture II, poly[(*R*)-**11**] with DP = 11, M_w/M_n = 1.21 and poly[(*S*)-**11**] with DP = 11, M_w/M_n = 1.26; and polymer mixture III, poly[(*R*)-**11**] with DP = 17.0, M_w/M_n = 1.27 and poly[(*S*)-**11**] with DP = 16, M_w/M_n = 1.23.

The characterization polymer mixture I is summarized in Table 4 and the corresponding phase diagrams are presented in Figure 9. All mixtures display enantiotropic S_A and S_C* phases as well as a crystalline phase. The structural units of these polymers are isomorphic[20] within their smectic and crystalline phases. The isotropization temperatures display an almost linear dependence on composition while the S_C*−S_A transition has a slight negative curvature on all scans. A more pronounced negative curvature is observed for the K−S_C* transition on the first and second heating scan, corresponding to the formation of a nonideal solution due to a homochiral preference. The only notable feature from these phase diagrams is the upward curvature of the S_C*−K transition from the cooling scan which shows a positive curvature (chiral recognition effect) with a deviation of up to 4.7 °C from the calculated value.

The characterization of polymer mixture II is summarized in Table 5 while the corresponding phase diagrams are shown in Figure 10. On the first heating scan all mixtures display several crystalline phases followed by a S_A phase. The S_A−I transition temperature shown an almost linear dependence on composition while the crystalline transitions exhibit nonideal solution behavior with a homochiral preference. On the second heating scan, for compositions between 0.2 and 0.8, the crystalline phase is depressed to such an extent that an unidentified smectic phase (S_3) is uncovered in the mixture prior to the formation of the S_A phase. The S_A−I transition shows again an almost linear dependence on composition. The cooling scan generates a more complex phase diagram. The I−S_A transition temperature shows a slight upward curvature with a positive deviation of up to 0.5 °C from the calculated value. This is indicative of chiral recognition in the S_A phase and heterochiral interactions. For compositions between 0.3 and 0.7 the S_A phase is followed by the S_3 phase, while for all other compositions it is followed by the S_C* (S_1) phase. The S_A−S_3 and S_A−S_C* transitions show a negative curvature and nonideal solution behavior. On further cooling, the S_3 phase generates a higher order unidentified S_2 phase. The dependence of the S_3−S_2 transition temperature shows a positive deviation of up to 4.6 °C (calculated assuming virtual S_2 in homopolymers) or 2.9 °C (from the 0.1 and 0.9 compositions) from the calculated values. This is evidence of chiral recognition in the S_2 phase. The dependence of crystalline melting temperature on composition corresponds to the formation of a racemate. The S_A phase is enantiotropic for all compositions while the S_3 phase is enantiotropic for the 0.3−0.7 compositions and monotropic for the 0.2 and 0.8 compositions. The S_C* (S_1) and S_2 phases are monotropic.

The characterization of polymer mixture III is given in Table 6. The DSC thermograms are presented in Figure 11 , and the corresponding phase diagrams are shown in Figure 12. All mixtures display an enantiotropic S_A phase. The dependence of the isotropization temperature on composition is almost linear on all scans. On the first heating scan, several crystalline phases precede the S_A phase, and the dependence of the melting temperatures on composition displays a nonideal solution behavior with negative deviation. On the second heating scan, for the 0.1 and 0.9 compositions the crystalline phase melts into the S_3 phase which is followed by the S_C* (S_1) phase and then the S_A phase. For compositions between 0.2 and 0.8 an additional S_2 phase is observed between the crystal phase and the S_3 phase. However the S_C* phase is suppressed for these compositions. The dependence of the S_3−S_A transition temperature on composition shows a slight downward curvature. The same trend but more pronounced is observed for the K−S_2 transition. A remarkable feature

(20) Percec, V.; Tsuda, Y. *Polymer* **1991**, *32*, 661.

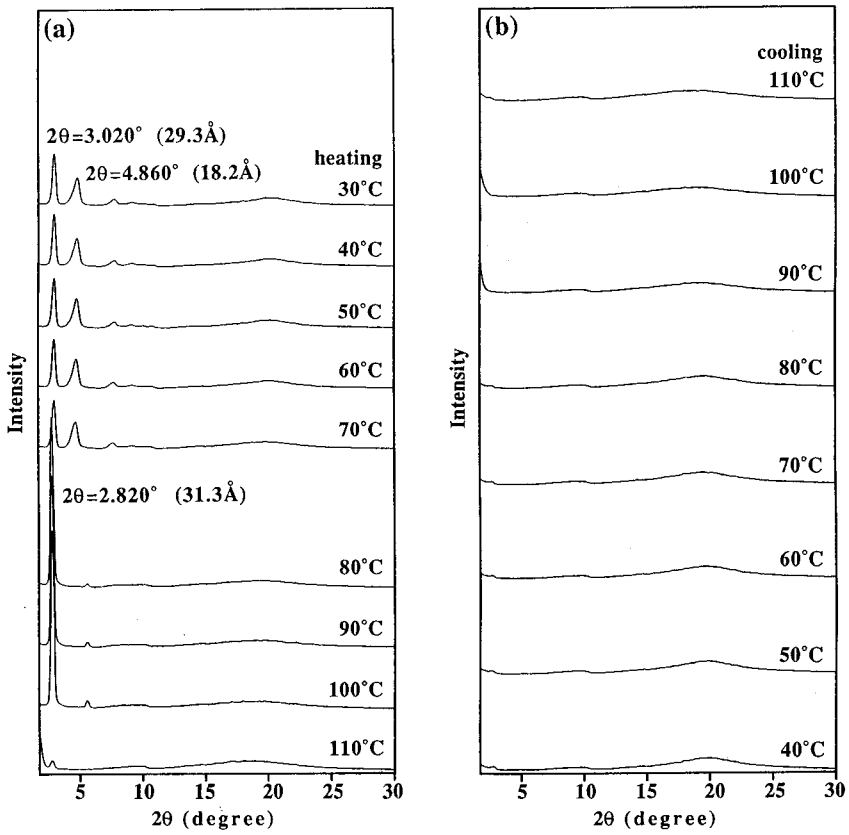

Figure 8. X-ray diffraction diagrams of poly[(*R*)-**11**] (DP = 17.0): (a) data from the heating scans and (b) data from the cooling scans.

Table 4. Characterization of the Binary Mixtures of Poly[(*R*)-11] (DP = 7, M_w/M_n = 1.26) with Poly[(*S*)-11] (DP = 7, M_w/M_n = 1.28) (Polymer Mixture I)

poly[(R)-**11**]/poly[(S)-**11**] (mol)/(mol)	phase transitions (°C) and corresponding enthalpy changes (kcal/mru)[a]	
	heating	cooling
0/100	K 39.2 (3.34) S_A 72.8 (1.11)	I 67.7 (−1.12) S_A 36.7 (−0.08) S_1 2.4 (−1.15) K
	K 29.2 (2.09) S_1 40.6 (0.07) S_A 73.0 (1.11) I	
10.0/90.0	K 35.2 (2.52) S_1 40.4 (0.06) S_A 72.4 (1.13) I	I 67.7 (−1.11) S_A 36.0 (−0.07) S_1 3.5 (−1.18) K
	K 28.3 (1.89) S_1 39.9 (0.06) S_A 72.9 (1.09) I	
20.3/79.7	K 34.5 (2.32) S_1 40.1 (0.08) S_A 72.5 (1.03) I	I 68.2 (−1.07) S_A 36.0 (−0.06) S_1 5.5 (−1.26) K
	K 27.3 (1.68) S_1 39.8 (0.06) S_A 73.2 (1.05) I	
40.0/60.0	K 33.5 (2.45) S_1 40.6 (0.07) S_A 73.0 (1.10) I	I 68.7 (−1.10) S_A 36.6 (−0.07) S_1 7.8 (−1.55) K
	K 25.6 (1.82) S_1 40.0 (0.06) S_A 73.5 (1.09) I	
50.1/49.9	K 33.8 (2.52) S_1 40.6 (0.07) S_A 73.7 (1.10) I	I 69.2 (−1.10) S_A 36.7 (−0.07) S_1 8.2 (−1.50) K
	K 25.7 (1.85) S_1 40.2 (0.06) S_A 74.0 (1.10) I	
60.5/39.5	K 33.6 (2.66) S_1 40.9 (0.08) S_A 73.4 (1.14) I	I 69.3 (−1.15) S_A 37.1 (−0.07) S_1 8.3 (−1.57) K
	K 26.2 (1.99) S_1 40.6 (0.07) S_A 73.9 (1.13) I	
80.5/19.5	K 34.3 (2.58) S_1 41.4 (0.09) S_A 73.9 (1.07) I	I 69.7 (−1.09) S_A 37.3 (−0.06) S_1 6.4 (−1.42) K
	K 28.5 (1.82) S_1 41.0 (0.05) S_A 74.4 (1.09) I	
89.5/10.5	K 34.9 (2.77) S_1 41.7 (0.09) S_A 74.2 (1.13) I	I 69.9 (−1.15) S_A 37.8 (−0.07) S1 5.4 (−1.28) K
	K 29.7 (1.98) S_1 41.5 (0.06) S_A 74.4 (1.12) I	
100/0	K 39.5 (3.25) S_A 74.6 (1.09)	I 70.0 (−1.14) S_A 38.7 (−0.07) S_1 4.4 (−1.24) K
	K 29.6 (2.06) S_1 42.4 (0.07) S_A 75.0 (1.12) I	

[a] Data on the first line are from first heating and cooling scans. Data on the second line are from second heating scan. Heating and cooling rates are 10 °C/min.

of this phase diagram is the upward curvature of the S_2-S_3 transition with a positive deviation of up to 2.9 °C from the calculated value. On the cooling scan, the $I-S_A$ transition is almost linear vs composition while the $S_C^*-S_A$ and respectively S_3-S_A transitions show a slight negative curvature. The S_C^* (S_1) phase is observed only for the 0.1, 0.2, 0.8, and 0.9 compositions. Therefore, it is monotropic for the 0.2 and 0.8 compositions and enantiotropic for the 0.1 and 0.9 compositions. The $S_3-S_C^*$ transition temperature increases sharply with decreasing optical purity and becomes virtual for the 0.3−0.7 compositions. The S_2-K transition shows the features corresponding to the formation of a racemate. Again, the S_2-S_3 transition displays an upward curvature with a positive deviation of up to 2.4 °C from the theoretical value.

The behavior of the S_1 phase is very similar to that of an antiferroelectric phase reported by Goodby[4d,e] in that both S_1 and antiferroelectric phases are observed only for an enantiomeric mixture with a high optical purity. The fact that the bi- or multilayer structure was suggested in the X-ray analysis is consistent with this

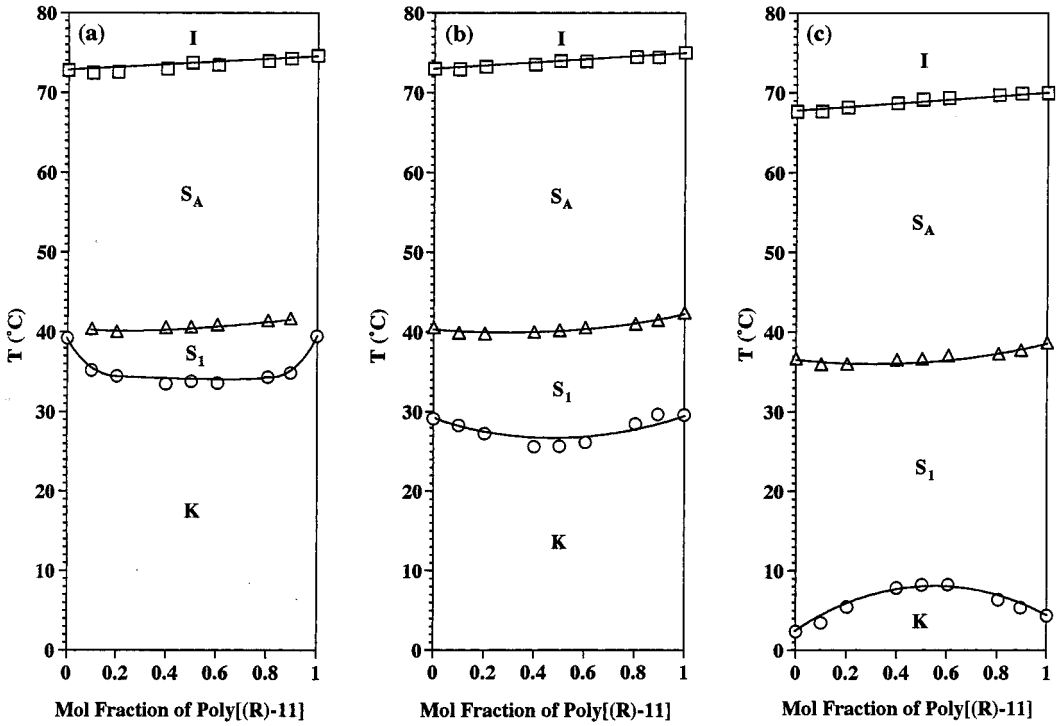

Figure 9. Dependence of phase transition temperatures on the composition of polymer mixture I [poly[(*R*)-**11**] (DP = 7) and poly[(*S*)-**11**] (DP = 7)]: (a) data from the first heating scans; (b) data from the second heating scans; and (c) data from the first cooling scans.

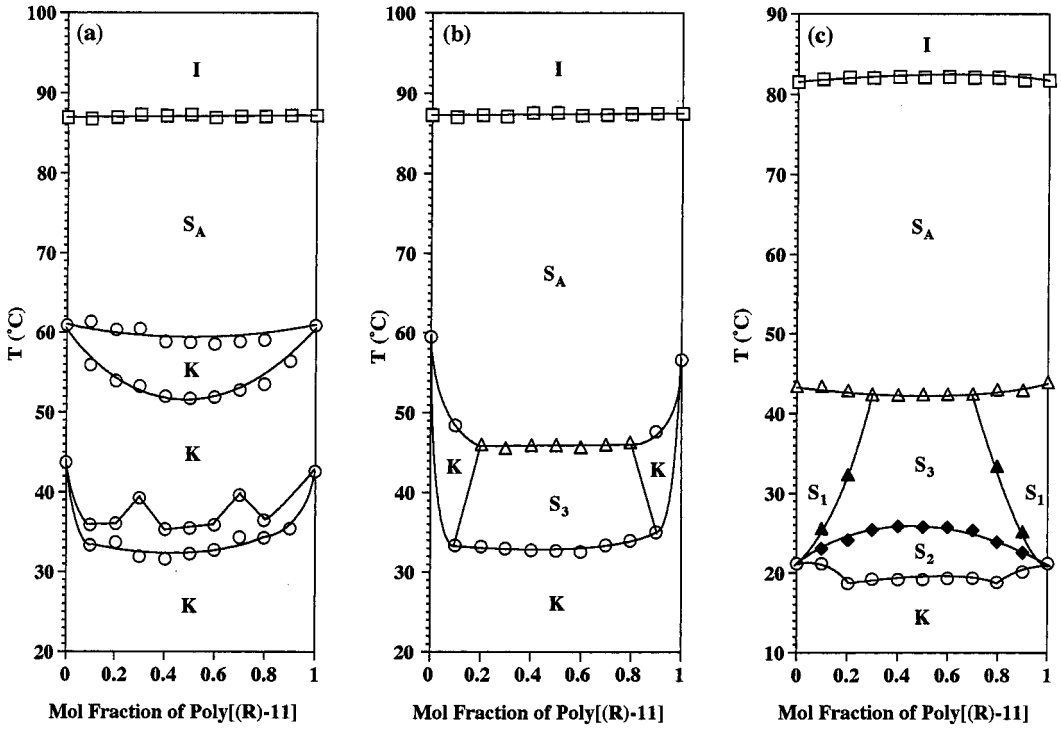

Figure 10. Dependence of phase transition temperatures on the composition of polymer mixture II [poly[(*R*)-**11**] (DP = 10) and poly[(*S*)-**11**] (DP = 11)]: (a) data from the first heating scans; (b) data from the second heating scans; and (c) data from the first cooling scans.

antiferroelectric-like behavior of the S_1 phase.[22] However, it was reported[4,21] that the antiferroelectric phase always appears in the lower temperature vicinity of the normal S_C* phase, while, in the current study, the S_3 phase is formed as a higher order (lower temperature) phase than the S_1 phase and the smectic phase corresponding to the normal S_C* phase is not observed in the

(21) (a) Skarp, K.; Andersson, G.; Lagerwall, S. T.; Kapitza, H.; Poths, H.; Zentel, R. *Ferroelectrics* **1991**, *122*, 127. (b) Scherowsky, G.; Kühnpast, K.; Springer, J. *Makromol. Chem., Rapid Commun.* **1991**, *12*, 381. (c) Bömelburg, J.; Heppke, G.; Hollidt, J. *Makromol. Chem., Rapid Commun.* **1991**, *12*, 483. (d) Nishiyama, I.; Goodby, J. W. *J. Mater. Chem.* **1993**, *3*, 169.

(22) Mensinger, H.; Biswas, A.; Poths, H. *Macromolecules* **1992**, *25*, 3156.

Table 5. Characterization of the Binary Mixtures of Poly[(*R*)-11] (DP = 11, M_w/M_n = 1.21) with Poly[(*S*)-11] (DP = 11, M_w/M_n = 1.26) (Polymer Mixture II)

poly[(*R*)-**11**]/poly[(*S*)-**11**] (mol)/(mol)	phase transitions (°C) and corresponding enthalpy changes (kcal/mru)[a]	
	heating	cooling
0/100	K 43.8 (3.35) K 60.9 (†[b]) S_A 86.9 (0.94) I K 59.5 (1.88) S_A 87.3 (0.92) I	I 81.5 (−0.94) S_A 43.5 (−0.07) S_1 21.2 (−1.44) K
9.9/90.1	K 33.4 (0.80) K 35.9 (†[b]) K 55.9 (1.52) K 61.4 (†[b]) S_A 86.8 (0.96) I K 33.4 (0.74) K 48.4 (1.43) S_A 87.0 (0.92) I	I 81.9 (−0.96) S_A 43.4 (−0.07) S_1 25.6 (†[b]) S_3 23.1 (†[b]) S_2 21.2 (−1.48) K
20.3/79.7	K 33.7 (0.97) K 36.0 (†[b]) K 54.0 (1.80) K 60.3 (†[b]) S_A 87.0 (0.96) I K 33.2 (1.34) S_3 46.0 (0.08) S_A 87.3 (0.93) I	I 82.1 (−0.96) S_A 42.9 (−0.07) S_1 32.4 (−0.01) S_3 24.2 (−0.27) S_2 18.7 (−1.01) K
29.9/70.1	K 31.9 (0.91) K 39.3 (†[b]) K 53.3 (1.99) K 60.5 (†[b]) S_A 87.3 (0.94) I K 33.0 (1.41) S_3 45.6 (0.06) S_A 87.1 (0.91) I	I 82.1 (−0.94) S_A 42.4 (−0.06) S_3 25.4 (−0.23) S_2 19.2 (−1.11) K
40.2/59.8	K 31.6 (0.82) K 35.3 (†[b]) K 52.0 (1.79) K 58.9 (†[b]) S_A 87.2 (0.97) I K 32.8 (1.54) S_3 45.9 (0.07) S_A 87.6 (0.95) I	I 82.2 (−0.98) S_A 42.4 (−0.06) S_3 25.9 (−0.28) S_2 19.2 (−1.10) K
50.1/49.9	K 32.3 (†[b]) K 35.5 (0.72) K 51.8 (2.06) K 58.8 (†[b]) S_A 87.3 (0.88) I K 32.7 (1.62) S_3 46.0 (0.07) S_A 87.6 (0.98) I	I 82.1 (−0.99) S_A 42.4 (−0.06) S_3 25.8 (−0.26) S_2 19.2 (−1.19) K
59.9/40.1	K 32.8 (0.73) K 35.9 (†[b]) K 51.9 (2.00) K 58.6 (†[b]) S_A 87.0 (0.96) I K 32.6 (1.69) S_3 45.7 (0.07) S_A 87.2 (0.97) I	I 82.2 (−0.97) S_A 42.5 (−0.06) S_3 25.7 (−0.28) S_2 19.3 (−1.12) K
69.9/30.1	K 34.4 (0.94) K 39.7 (†[b]) K 52.8 (2.04) K 58.9 (†[b]) S_A 87.1 (0.94) I K 33.4 (1.54) S_3 46.0 (0.06) S_A 87.3 (0.92) I	I 82.1 (−0.95) S_A 42.5 (−0.07) S_3 25.3 (−0.27) S_2 19.4 (−1.07) K
79.6/20.4	K 34.3 (0.98) K 36.5 (†[b]) K 53.6 (2.01) K 59.1 (†[b]) S_A 87.1 (0.99) I K 34.0 (1.50) S_3 46.3 (0.10) S_A 87.4 (0.96) I	I 82.1 (−0.98) S_A 43.0 (−0.06) S_1 33.4 (−0.01) S_3 23.9 (−0.24) S_2 18.8 (−1.09) K
89.9/10.1	K 35.4 (0.88) K 56.4 (1.72) S_A 87.2 (0.99) I K 35.0 (0.83) K 47.6 (0.96) S_A 87.5 (0.96) I	I 81.8 (−0.98) S_A 43.0 (−0.07) S_1 25.2 (†[b]) S_3 22.6 (†[b]) S_2 20.2 (−1.42) K
100/0	K 42.6 (3.39) K 60.9 (†[b]) S_A 87.2 (0.97) I K 56.6 (1.88) S_A 87.5 (0.96) I	I 81.7 (−0.98) S_A 44.0 (−0.06) S_1 21.2 (−1.47) K

[a] Data on the first line are from first heating and cooling scans. Data on the second line are from second heating scan. Heating and cooling rates are 10 °C/min. [b] Overlapped peak.

Table 6. Characterization of the Binary Mixtures of Poly[(*R*)-11] (DP = 17, M_w/M_n = 1.27) with Poly[(*S*)-11] (DP = 16, M_w/M_n = 1.23) (Polymer Mixture III)

poly[(*R*)-**11**]/poly[(*S*)-**11**] (mol)/(mol)	phase transitions (°C) and corresponding enthalpy changes (kcal/mru)[a]	
	heating	cooling
0/100	K 45.0 (1.14) K 66.5 (2.60) S_A 93.6 (0.96) I K 59.7 (2.13) S_A 93.7 (0.93) I	I 88.0 (−0.94) S_A 46.3 (−0.07) S_1 32.9 (−0.35) S_2 27.9 (−1.27) K
9.8/90.2	K 35.0 (0.39) K 59.9 (2.24) K 65.6 (†[b]) S_A 93.7 (0.93) I K 38.2 (1.08) S_3 45.0 (†[b]) S_1 49.3 (0.07) S_A 93.8 (0.89) I	I 88.3 (−0.89) S_A 45.9 (−0.06) S_1 36.1 (†[b]) S_3 33.4 (−0.33) S_2 21.9 (−0.93) K
19.9/80.1	K 33.3 (0.58) K 58.9 (2.05) K 64.6 (†[b]) S_A 93.7 (0.96) I K 36.5 (1.58) S_2 38.7 (†[b]) S_3 48.8 (0.06) S_A 94.1 (0.90) I	I 88.5 (−0.91) S_A 45.5 (−0.07) S_1 42.0 (†[b]) S_3 34.4 (−0.32) S_2 22.4 (−0.94) K
30.9/69.1	K 35.4 (0.58) K 39.7 (†[b]) K 58.4 (2.13) K 64.3 (†[b]) S_A 94.1 (0.87) I K 36.3 (1.48) S_2 40.0 (†[b]) S_3 48.9 (0.05) S_A 94.4 (0.85) I	I 88.8 (−0.86) S_A 45.2 (−0.06) S_3 35.8 (−0.29) S_2 23.0 (−0.85) K
40.1/59.9	K 33.6 (0.57) K 58.3 (2.14) S_A 94.1 (0.95) I K 36.0 (1.68) S_2 40.2 (†[b]) S_3 48.7 (0.06) S_A 94.4 (0.92) I	I 88.8 (−0.91) S_A 45.1 (−0.06) S_3 36.0 (−0.38) S_2 22.9 (−1.03) K
50.2/49.8	K 32.4 (0.55) K 40.6 (†[b]) K 58.6 (1.61) S_A 94.2 (0.99) I K 36.0 (1.84) S_2 40.0 (†[b]) S_3 48.4 (0.06) S_A 94.3 (0.97) I	I 88.8 (−0.96) S_A 45.0 (−0.06) S_3 35.9 (−0.41) S_2 23.2 (−1.10) K
59.5/40.5	K 32.9 (0.65) K 58.0 (2.62) K 64.5 (†[b]) S_A 94.3 (0.94) I K 36.0 (1.76) S_2 40.4 (†[b]) S_3 48.9 (0.07) S_A 94.6 (0.92) I	I 89.2 (−0.94) S_A 45.7 (−0.06) S_3 36.5 (−0.38) S_2 23.4 (−1.03) K
70.1/29.9	K 35.7 (†[b]) K 60.0 (3.03) S_A 94.8 (0.91) I K 36.9 (1.52) S_2 40.3 (†[b]) S_3 49.1 (0.05) S_A 94.9 (0.88) I	I 89.2 (−0.87) S_A 45.3 (−0.06) S_3 35.9 (−0.33) S_2 23.0 (−0.94) K
80.1/19.9	K 36.1 (0.62) K 59.6 (3.03) K 65.5(†[b]) S_A 94.5 (1.08) I K 36.8 (1.97) S_2 39.7 (†[b]) S_3 49.3 (0.08) S_A 94.9 (1.07) I	I 89.3 (−1.08) S_A 45.9 (−0.07) S_1 43.0 (†[b]) S_3 35.1 (−0.40) S_2 22.9 (−1.20) K
89.9/10.1	K 33.0 (0.71) K 36.8 (†[b]) K 60.8 (2.76) K 66.4 (†[b]) S_A 94.5 (1.11) I K 39.1 (1.78) S_3 46.5 (†[b]) S_1 49.9 (0.10) S_A 94.9 (1.08) I	I 89.3 (−1.10) S_A 46.4 (−0.07) S_1 38.4 (−0.01) S_3 34.3 (−0.32) S_2 22.1 (−1.19) K
100/0	K 43.1 (†[b]) K 65.8 (3.58) S_A 94.6 (0.95) I K 62.1 (2.08) S_A 94.8 (0.92) I	I 89.3 (−0.94) S_A 47.2 (−0.07) S_1 34.1 (−0.35) S_2 28.6 (−1.27) K

[a] Data on the first line are from first heating and cooling scans. Data on the second line are from second heating scan. Heating and cooling rates are 10 °C/min. [b]Overlapped peak.

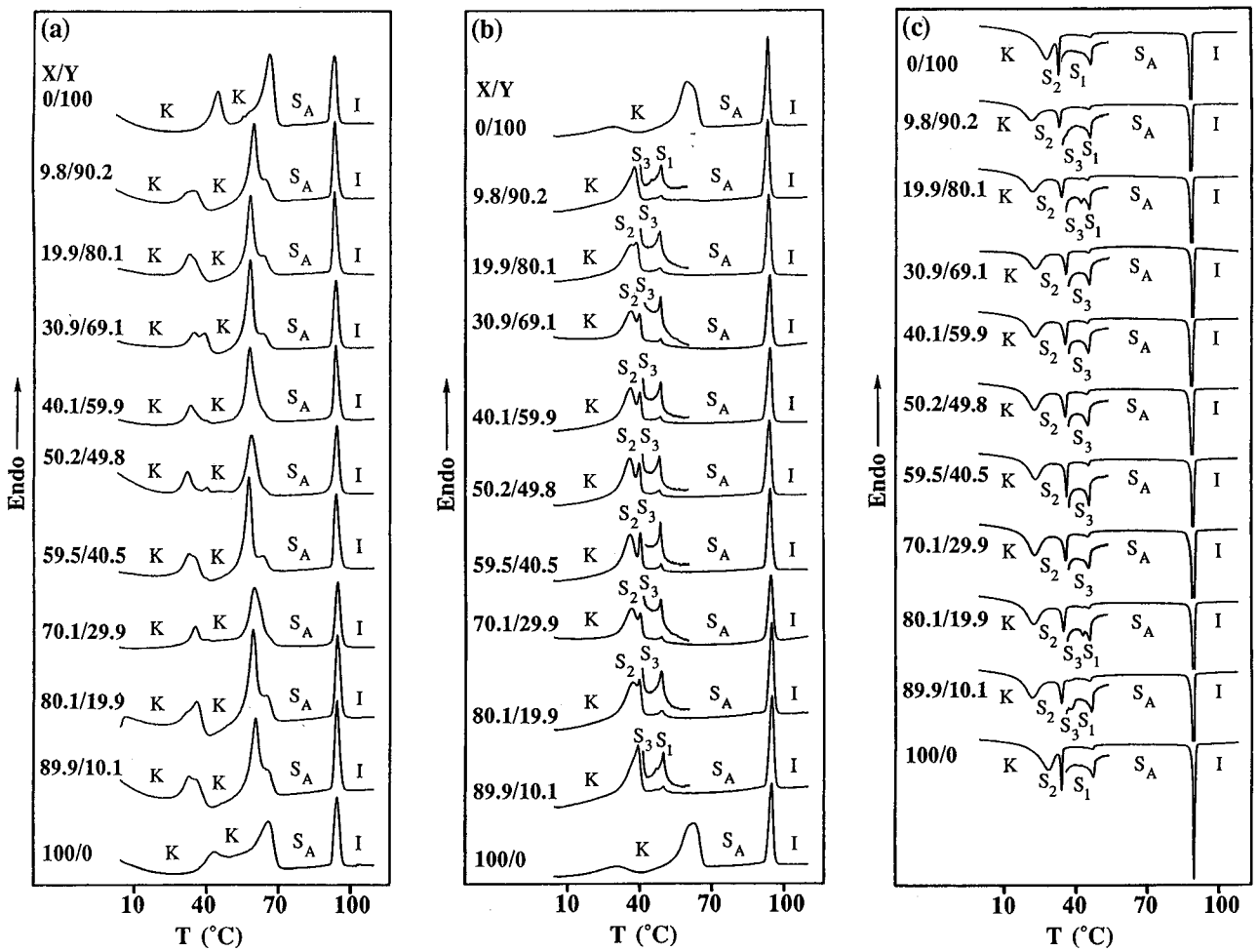

Figure 11. DSC thermograms (10 °C/min) of polymer mixture III [poly[(*R*)-**11**] (DP = 17.0) and poly[(*S*)-**11**] (DP = 16)]: (a) first heating scans; (b) second heating scans; and (c) first cooling scans.

DSC analysis. Electrooptical measurements[21] and X-ray scattering experiments[22] would be required to confirm the nature of the S_1 and S_3 phases.

Figure 13 displays the dependence of the difference (ΔT) between the experimental and calculated (Schröder−van Laar) values of the I−S_A transition temperature (collected from the first cooling scans of the monomer mixture and of the three sets of polymer mixtures) on composition. Regardless of the fluctuation of the data points, the following trends are observed: (a) monomer mixtures show relatively higher deviation than the polymer mixtures and (b) medium molecular weight polymer mixtures (polymer mixture II) show larger deviations than the other two polymer mixtures. A similar trend was observed for the polymer mixtures derived from (*R*)- and (*S*)-2-chloro-4-methylpentyl 4′-[[8-(vinyloxy)octyl]oxy]biphenyl-4-carboxylate enantiomers, which have a shorter alkyl chain than the monomers used in this study.[12b] The maximum deviation is achieved by the polymer mixtures with DP ∼ 10 in both undecanyl and octyl alkyl systems and this degree of polymerization seems to represent the optimum molecular weight that favors the largest chiral molecular recognition in the S_A phase of these polymers. For polymers whose molecular weight is less than the optimum value, the polymer backbone effect enhances the chiral molecular recognition between the two enantiomeric side chain structural units through a cooperative effect.[23,24] However, when the molecular weight of the polymer exceeds this optimum value, the polymer backbone decreases and finally cancels the chiral molecular recognition.

Copolymerization of (*R*)-11 and (*S*)-11. Copolymerization of (*R*)-**11** with (*S*)-**11** was performed in the composition range of (*R*)-**11**/(*S*)-**11** = 50/50−100/0. All (poly[[(*R*)-**11**]-*co*-[(*S*)-**11**]]) copolymers were synthesized with DP ∼ 13. Since the transition temperatures of polymers are strongly dependent on their molecular weights, it is essential to synthesize polymers having identical molecular weights to compare their transition temperatures. This can be achieved only by a living polymerization. The copolymerization results are listed in Table 7. The yields reported in Table 7 are lower than quantitative due to the polymer loss during the purification process. However, all conversions were quantitative and therefore, the copolymer composition is identical to that of the monomer feed.[13] The DSC scans and

(23) (a) Ciardelli, F.; Salvadori, P. *Pure Appl. Chem.* **1985**, *57*, 931. (b) Selegny, E., Ed. *Optically Active Polymers*; D. Reidel Publishing Co.: Dordrecht, The Netherlands, 1979. (c) Matsuzaki, K.; Watanabe, T. *Makromol. Chem.* **1971**, *146*, 109.

(24) (a) Pugh, C.; Rodriguez-Parada, J.; Percec, V. *J. Polym. Sci: Part A: Polym. Chem.* **1986**, *24*, 747. (b) Percec, V.; Schild, H. G.; Rodriguez-Parada, J. M.; Pugh, C. *J. Polym. Sci: Part A: Polym. Chem.* **1988**, *26*, 935.

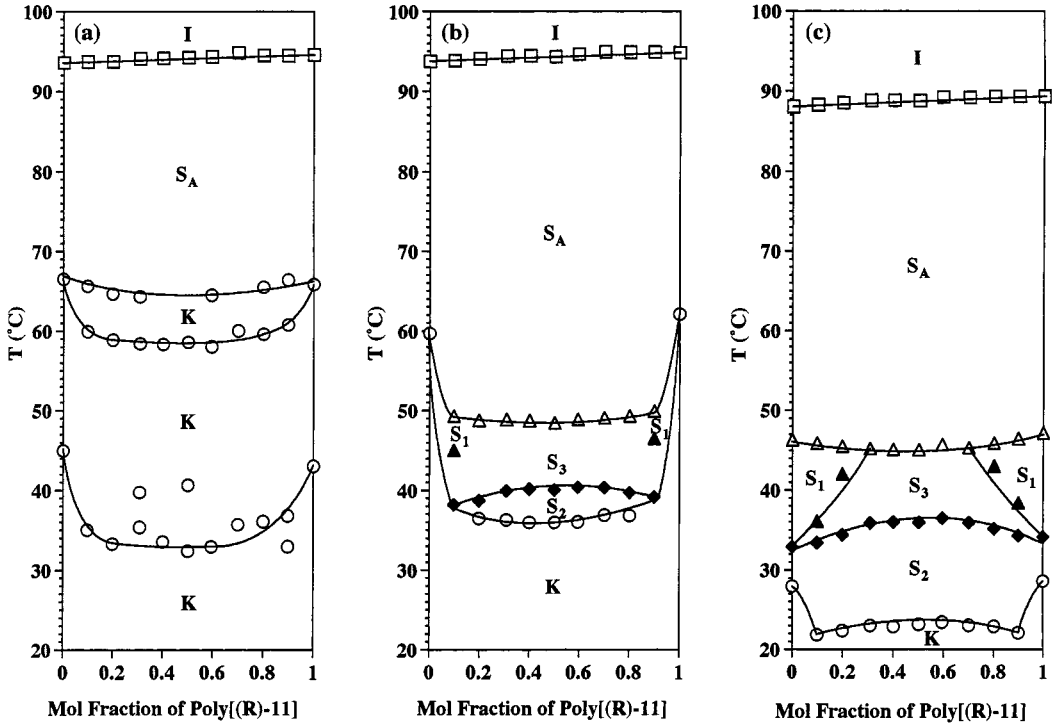

Figure 12. Dependence of phase transition temperatures on the composition of polymer mixture III [poly[(*R*)-**11**] (DP = 17.0) and poly[(*S*)-**11**] (DP = 16)]: (a) data from the first heating scans; (b) data from the second heating scans; and (c) data from the first cooling scans.

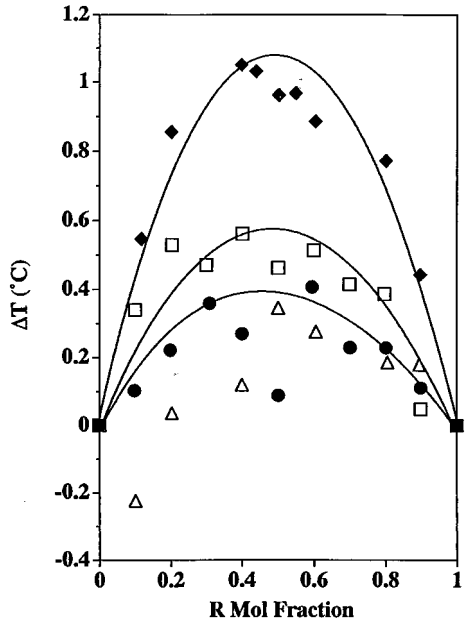

Figure 13. The dependence of the difference between the experimental and calculated values of the S_A−I transition temperatures on composition. Data from the first cooling scan.

the corresponding phase diagrams of these copolymers are presented in Figure 14 and respectively Figure 15. All copolymers display an enantiotropic S_A phase. On the first heating scan two crystalline phases are observed. The lower temperature crystalline phase depends little on composition while the stability of the higher temperature crystalline phase decreases toward the 50/50 copolymer. Therefore by copolymerization the stability of the S_A phases increases. Copolymerization is a known technique for depressing crystalline phases and uncovering LC phases.[25] Therefore, on the second heating scan while the lower temperature crystalline phase is still observed, the higher temperature crystalline phase occurs only for compositions between 0.8 and 1. For compositions between 0.7 and 0.5 the crystal phase melts into the S_2 phase that generates the S_C* (S_1) phase and subsequently the S_A phase. On the cooling scan, the S_A phase is followed by the S_C* (S_1) phase and subsequently by the S_2 phase and the crystal phase for all compositions. The S_2 phase is enantiotropic for compositions from 0.5 to 0.7 while the S_C* (S_1) phase is enantiotropic for compositions between 0.5 and 0.9. On all scans the isotropization temperature appears to display a small upward curvature. A comparison between the mixtures of homopolymers and copolymers in terms of chiral molecular recognition effects is more difficult to make as one should consider the chiral interactions not only between chains but also along the same chain. The S_3 phase is totally suppressed by the S_1 phase in the case of copolymers which are more disordered systems. It is possible that the random sequence distribution of the copolymer disrupts the side chain arrangements necessary for the formation of the S_1 mesophase. X-ray analysis is required again to support this speculation.

Conclusions

The chiral molecular recognition effect has a very complex dependence of the nature and size of the substituents at the chiral center and on the molecular weight. A comprehensive comparison is therefore difficult to make as the nature and stability of the phases

(25) Percec, V. In *Handbook of Liquid Crystal Research*; Collins, P. J., Patel, S., Eds.; Oxford University Press: Oxford, 1997; pp 259−346.

displayed by the systems under investigation depend on monomer structure, on DP, and on composition. Therefore each molecular weight or monomer structure may favor chiral recognition in a different phase for a certain composition. For example the I−S_A transition of the monomers for the system based on (*R*)- and (*S*)-2-chloro-4-methylpentyl 4′-[[8-(vinyloxyl)octyl]oxy]biphenyl-4-carboxylate enantiomer pairs ((*R*)-**8** and (*S*)-**8**)[12b] (with an identical structure except that the length of the alkyl group is different, i.e., undecanyl vs octyl) has a maximum positive deviation from the calculated values of 0.4 °C while the systems in this work show a positive deviation of 1 °C. For the corresponding polymers, the systems based on an octyl chain display a positive deviation of up to 1.3 °C while the systems based on the undecanyl chain show a positive deviation of up to 0.5 °C for the same transition. On the other hand, the side chain liquid crystalline polymers based on (*R*)-**11** and (*S*)-**11** containing a longer spacer,[26] display a much richer polymorphism and more ordered phases. For these systems, chiral recognition is observed in various phases (depending on molecular weight) not only from the I−S_A transition, but also from the K−I, S_C*−K, and S_3−S_2 transitions.

The phase behavior of the polymer mixtures is unique in the point that the polymer mixtures with a high optical purity exhibit a different phase sequence from those with a low optical purity. With respect to the polymer mixtures with DP > 10, the S_C* (S_1) phase is observed between the S_A and S_2 phases when their optical purities are higher than 80%, whereas the S_3 phase replaces the S_1 phase when their optical purities are below 80%. This behavior is in contrast to that of the corresponding copolymers between (*R*)-**11** and (*S*)-**11**, since the copolymers showed continuous dependence on the composition for all mesophases and the dependence of the phase sequence on the optical purity is not observed. It can be presumed that the random sequence distribution of the copolymer is responsible for this difference between the polymer mixture system and the copolymer system. The precise interpretation of these phase behaviors requires a complete characterization by X-ray scattering experiments.

With regard to the S_A−I transition of the polymer mixtures, a dependence of chiral molecular recognition on polymer molecular weight is observed. This dependence implies the existence of an optimum molecular weight that favors the largest chiral molecular recognition in the S_A phase. The same molecular weight dependence was also obtained in the system with an octyl alkyl group.[12b] It should be noted that in the system in which chlorine atom is connected to the chiral center, the polymer backbone can play a role in enhancing the chiral molecular recognition, while, in the similar system in which a fluorine atom is connected to the chiral center, the polymer backbone only depresses the chiral recognition.[12c] This difference is probably caused by the differences in both the atomic size and dipole moment between the chlorine and fluorine atoms.

In contrast to the small (1 °C) chiral molecular recognition in the S_A phase, the dependence of the K−I, S_C*−K, and S_3−S_2 transitions on composition demon-

Table 7. Cationic Copolymerization of (*R*)-11 with (*S*)-11 and Characterization of the Resulting Polymers[a]

[(*R*)-**11**]/[(*S*)-**11**] (mol/mol)	polymer yield (%)	M_n × 10^{-3}	M_w/M_n	DP	phase transitions (°C) and corresponding enthalpy changes (kcal/mru)[b]	
					heating	cooling
50/50	68.9	6.72	1.20	13	K 40.9 (f[c]) K 57.6 (3.29) S_A 92.1 (0.89) I K 30.9 (1.03) S_2 33.5 (f[c]) S_1 47.2 (0.06) S_A 92.2 (0.88) I	I 86.6 (−0.89) S_A 43.9 (−0.06) S_1 29.6 (−0.25) S_2 18.7 (−0.86) K
60/40	72.5	6.67	1.20	13	K 41.5 (f[c]) K 57.6 (3.30) S_A 91.6 (0.89) I K 30.4 (1.04) S_2 32.1 (f[c]) S_1 46.8 (0.06) S_A 91.5 (0.88) I	I 86.1 (−0.89) S_A 43.4 (−0.06) S_1 28.6 (−0.25) S_2 18.5 (−0.89) K
70/30	74.3	6.88	1.19	13	K 39.7 (f[c]) K 59.5 (3.50) S_A 93.2 (0.89) I K 32.8 (1.06) S_2 34.9 (f[c]) S_1 48.1 (0.07) S_A 92.9 (0.89) I	I 87.4 (−0.89) S_A 44.6 (−0.07) S_1 31.1 (−0.26) S_2 19.2 (−0.94) K
80/20	69.5	6.71	1.20	13	K 40.1 (f[c]) K 60.0 (3.16) S_A 92.0 (0.89) I K 33.7 (0.87) S_1 48.2 (f[c]) K 51.2 (0.34) S_A 92.2 (0.88) I	I 86.2 (−0.88) S_A 44.6 (−0.05) S_1 29.0 (f[c]) S_2 19.0 (−1.16) K
90/10	67.2	6.77	1.20	13	K 40.2 (f[c]) K 62.3 (3.35) S_A 92.3 (0.88) I K 28.5 (0.50) K 54.8 (2.11) S_A 92.4 (0.87) I	I 86.6 (−0.90) S_A 45.3 (−0.07) S_1 30.1 (−0.31) S_2 26.2 (−1.20) K
100/0	70.1	6.72	1.18	13	K 40.3 (f[c]) K 64.2 (3.52) S_A 90.9 (0.90) I K 26.3 (0.40) K 60.9 (1.93) S_A 90.8 (0.89) I	I 85.3 (−0.91) S_A 45.6 (−0.07) S_1 28.3 (−0.32) S_2 24.8 (−1.20) K

[a] Polymerization temperature: 0 °C; polymerization solvent, methylene chloride; $[M]_o = [(R)\text{-}\mathbf{11}]+[(S)\text{-}\mathbf{11}] = 0.224$; $[M]_o/[I]_o = 20$; $[Me_2S]_o/[I]_o = 10$; polymerization time, 1 h. [b] Heating and cooling rates are 10 °C/min. Data on the first line are from first heating and cooling scans. Data on the second line are from second heating scan. [c] Overlapped peak.

(26) Pugh, C.; Kiste, A. L. *Prog. Polym. Sci.* **1997**, *22*, 601.

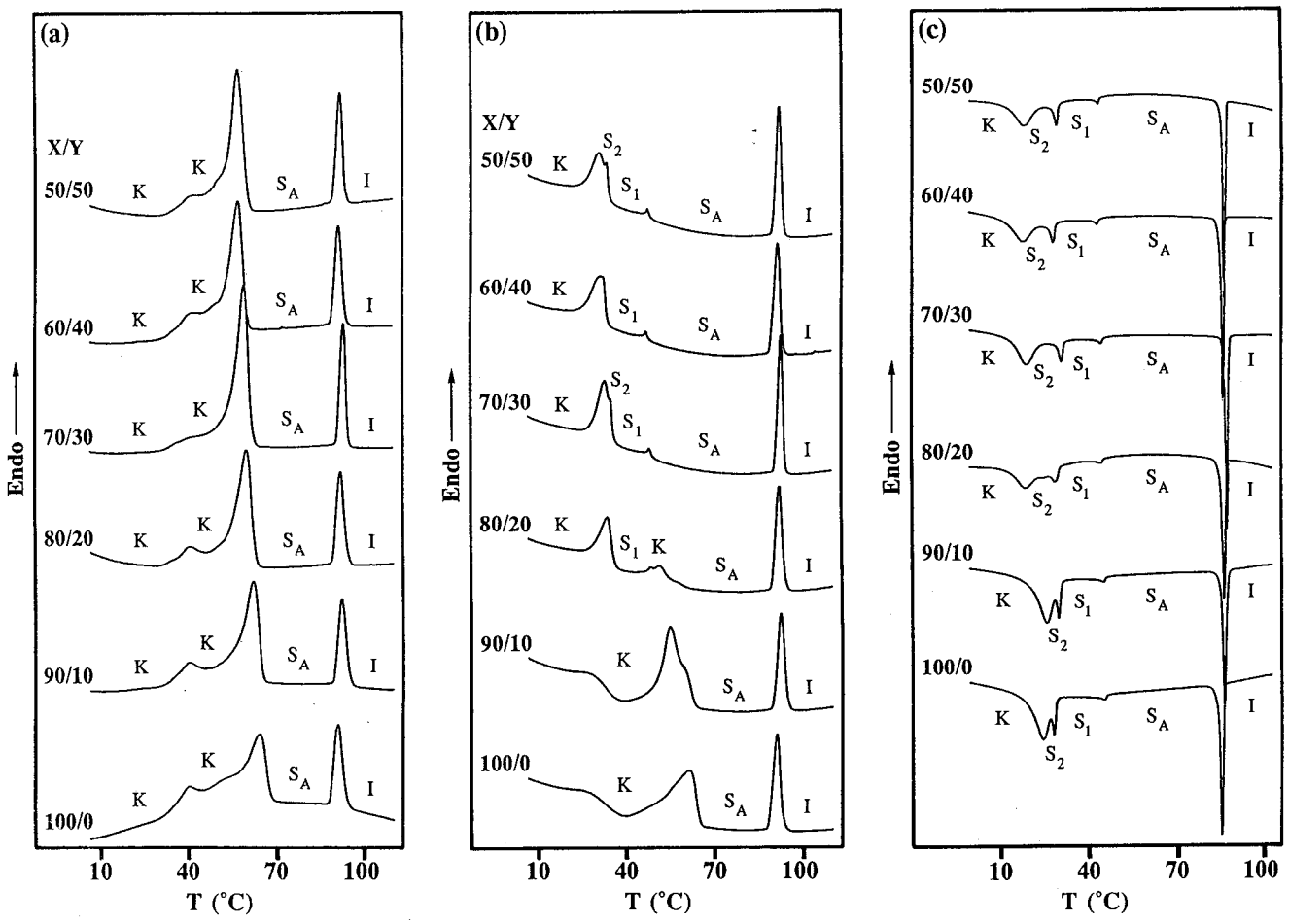

Figure 14. DSC thermograms (10 °C/min) of poly[[(*R*)-**11**]-*co*-[(*S*)-**11**]]X/Y with various compositions: (a) first heating scans; (b) second heating scans; and (c) first cooling scans.

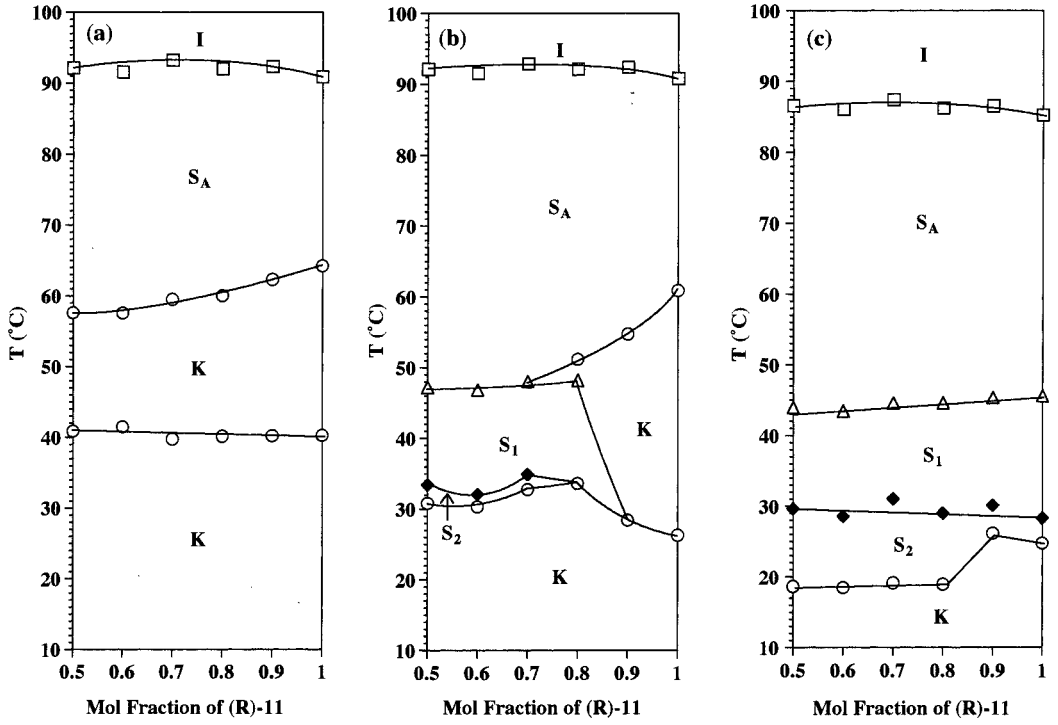

Figure 15. Dependence of the phase transition temperatures on the composition of poly[[(*R*)-**11**]-*co*-[(*S*)-**11**]] (DP = 13): (a) data from the first heating scans; (b) data from the second heating scans; and (c) data from the first cooling scans.

strate larger chiral molecular recognition effects in the corresponding phases. It is likely that the extent of chiral recognition is also dependent on the degree of order within the mesophase and higher order me-

sophase afford larger chiral molecular recognition effect. This may be due to the fact that specific chiral interactions may be less rotationally averaged with increasing mesophase order.

Experimental Section

Materials. L-Leucine [(*S*)−(+)-2-amino-4-methylpentanoic acid, 99%, Aldrich], D-leucine [(*R*)−(−)-2-amino-4-methylpentanoic acid, 99%, Aldrich], and borane·tetrahydrofuran complex (BH_3·THF, 1.0M solution in THF, Aldrich) were used as received.

Pyridine was heated overnight at 100 °C over KOH, distilled from KOH, and then stored over KOH. Dimethyl sulfoxide (DMSO) was heated overnight at 100 °C over CaH_2, distilled from CaH_2 under vacuum, and stored over molecular sieves (4 Å). Tetrahydrofuran (THF) was refluxed over $LiAlH_4$ for several days and distilled from $LiAlH_4$. Acetone was stored over anhydrous K_2CO_3 for several days, filtered and distilled.

CH_2Cl_2, used as polymerization solvent, was first washed with concentrated H_2SO_4 several times until the acid layer remained colorless, washed with water, dried over $MgSO_4$, refluxed over CaH_2, and freshly distilled under argon before each use. Dimethyl sulfide [$(CH_3)_2S$] used in polymerizations (Aldrich, anhydrous, 99+%, packed under nitrogen in Sure/Seal bottle) was used as received. Trifluoromethanesulfonic acid (CF_3SO_3H) used as polymerization initiator (Aldrich, 98%) was distilled under vacuum.

All other materials were commercially available and were used as received.

Techniques. ^{1}H NMR spectra were recorded on a Varian XL-200 (200 MHz) spectrometer.

Relative molecular weights of polymers were determined by gel permeation chromatography (GPC). GPC analyses were carried out with a Perkin-Elmer Series 10LC instrument equipped with an LC-100 column oven and a Nelson Analytical 900 Series data station. Measurements were made by using an UV detector, THF as solvent (1 mL/min, 40 °C), a set of PL gel columns of 5×10^2 and 10^4 Å, and a calibration plot constructed with polystyrene standards.

A Perkin-Elmer PC Series DSC-7 differential scanning calorimeter equipped with a TAC7/DX thermal analysis controller and calibrated with In and Zn standards to an accuracy of ±0.1 °C was used to determine the thermal transition temperatures, which were reported as the maxima and minima of their endothermic or exothermic peaks, respectively. Heating and cooling rates were 10 °C/min in all experiments.

X-ray diffraction measurements were performed with a Rigaku powder diffractometer. The monochromatized X-ray beam from Cu Kα radiation with a wavelength of 0.154 18 nm was used. A temperature controller was added to the X-ray apparatus for thermal measurements. The precision of the controller was ±0.5 °C in the temperature range studied. Measurements were performed both on heating and cooling scans at 2.5 °C/min and 10°/min scanning rates.

A Carl-Zeiss optical polarizing microscope equipped with a Mettler FP-82 hot stage and a Mettler FP-80 central processor was used to observe the thermal transitions and to analyze the anisotropic textures.

Synthesis of Monomers. Monomers (*R*)-**11** and (*S*)-**11** were synthesized from D-(*R*)-leucine and l-(*S*)-leucine, respectively according to the reaction pathway outlined in Scheme 1. The syntheses of compounds (*R*)/(*S*)-**2** through (*R*)/(*S*)-**6**,[12b] and compounds **5** and **7**[13b−e] were previously described.

(*R*)-2-Chloro-4-methylpentyl 4′-[[11-(Vinyloxy)undecanyl]oxy]biphenyl-4-carboxylate [(*R*)-11]. A mixture of (*R*)-**6** (3.00 g, 9.0 mmol), anhydrous K_2CO_3 (3.11 g, 22.5 mmol), and dry acetone (80 mL) was stirred at 60 °C under a nitrogen atmosphere for 2 h. To the resulting yellow solution was added a solution of **7** (2.77 g, 10.0 mmol) in dry DMSO (5.0 mL) and stirring was continued at 60 °C for 20 h. The mixture was poured into water, and the product was extracted into diethyl ether twice. The combined ethereal extracts were dried over anhydrous $MgSO_4$. The solvent was evaporated, and the remaining crude product was purified by column chromatography twice (silica gel; hexane−ethyl acetate 20:1) to yield a white solid (2.49 g, 52.3%), purity >99% (HPLC). The thermal transition temperatures are reported in Table 3. ^{1}H NMR ($CDCl_3$, TMS): δ 0.95 (d, J = 6.7 Hz, 3H, $(CH_3)_2CH-$), 0.99 (d, J = 6.7 Hz, 3H, $(CH_3)_2CH-$), 1.16−2.06 (m, 21H, $(CH_3)_2CHCH_2-$, $CH_2{=}CHOCH_2(CH_2)_9-CH_2O-$), 3.68 (t, J = 6.5 Hz, 2H, $CH_2{=}CHOCH_2-$), 3.98 (dd, J = 6.9 Hz, 1.7 Hz, 1H, $CH_2{=}CHO-$ *trans*), 4.01 (t, J = 6.5 Hz, 2H, $-CH_2OPh-$), 4.17 (dd, J = 14.4, 1.7 Hz, 1H, $CH_2{=}CHO-$ *cis*), 4.23−4.56 (m, 3H, $-CHClCH_2OCO-$), 6.48 (dd, J = 14.4, 6.9 Hz, 1H, $CH_2{=}CHO-$), 7.00 (d, J = 8.8 Hz, 2ArH, *ortho* to $-(CH_2)_{11}O-$), 7.57 (d, J = 8.8 Hz, 2ArH, *meta* to $-(CH_2)_{11}O-$), 7.65 (d, J = 8.3 Hz, 2ArH, *meta* to −COO−), 8.11 (d, J = 8.3 Hz, 2ArH, *ortho* to −COO−).

Cationic Polymerizations. Polymerizations and copolymerizations were carried out in a three-necked round-bottom flask equipped with a Teflon stopcock and rubber septa under an argon atmosphere at 0 °C for 1 h. All glassware was dried overnight at 140 °C. The monomer was further dried under vacuum overnight in the polymerization flask. After the flask was filled with argon, freshly distilled dry methylene chloride was added via a syringe and the solution was cooled to 0 °C. Dimethyl sulfide and trifluoromethanesulfonic acid were then added carefully via a syringe. The monomer concentration was about 0.224 M, and the dimethyl sulfide concentration was 10 times larger than that of trifluoromethanesulfonic acid. The polymer molecular weight was controlled by the monomer/initiator ($[M]_o/[I]_o$) ratio. After the polymerization was quenched with a mixture of NH_4OH and methanol (1:2), the reaction mixture was poured into methanol to give a white precipitate. The obtained polymer was purified by the reprecipitation by pouring its chloroform solution into methanol, and dried under vacuum.

Acknowledgment. Financial support by the Office of Naval is gratefully acknowledged.

CM990083M